NASA Technical Paper 1892

Computer Analysis of Flow Perturbations Generated by Placement of Choke Bumps in a Wind Tunnel

Richard L. Campbell

AUGUST 1981

NASA

NASA Technical Paper 1892

Computer Analysis of Flow Perturbations Generated by Placement of Choke Bumps in a Wind Tunnel

Richard L. Campbell
Langley Research Center
Hampton, Virginia

NASA
National Aeronautics
and Space Administration

Scientific and Technical
Information Branch

1981

SUMMARY

An inviscid analytical study has been conducted to determine the upstream flow perturbations caused by placing choke bumps in a wind tunnel. A computer program based on the stream-tube curvature method was used to calculate the resulting flow fields for a nominal free-stream Mach number range of 0.6 to 0.9. The choke bump geometry was also varied to investigate the effect of bump shape on the disturbance produced.

Results from the study indicate that a region of significant variation from the free-stream conditions exists upstream of the throat of the tunnel. The greatest upstream disturbance distance generally occurred along the tunnel center line and extended from a minimum of about 0.25 tunnel height ahead of the throat to a maximum of about 2.0 tunnel heights for the cases considered. The extent of the disturbance region was, as a rule, dependent on Mach number and the geometry of the choke bump. In general, the upstream disturbance distance decreased for increasing nominal free-stream Mach number and for decreasing length-to-height ratio of the bump. A polynomial-curve choke bump usually produced less of a disturbance than did a circular-arc bump, and going to an axisymmetric configuration (modeling choke bumps on all the tunnel walls) generally resulted in a lower upstream disturbance distance than with the corresponding two-dimensional case. Finally, for some of the circular-arc configurations, certain flow parameters could be estimated by using the throat geometry.

INTRODUCTION

In general, the noise level in the test sections of high subsonic and transonic wind tunnels has been observed to be high. (See ref. 1.) This disturbance level can affect the quality of aerodynamic measurements taken during testing at these Mach numbers and could actually prevent certain experiments, such as laminar flow control, from being successfully carried out. A specific example is the planned large-chord swept-wing laminar flow control experiment to be conducted in the Langley 8-Foot Transonic Pressure Tunnel. The current disturbance level in the test section is too high; therefore, a few methods of reducing the noise level have been proposed. One of these solutions, choking the tunnel at the downstream end of the test section, was the impetus for conducting this study.

A large portion of the noise in the test section at higher Mach numbers has been attributed to the diffuser section of the tunnel. A recent study (ref. 2), done in the Langley 8-Foot Transonic Pressure Tunnel, has shown that choking the tunnel at the downstream end of the test section produced a significant reduction in the overall noise level in the test section. The choking was accomplished by adding bumps (circular-arc shaped plates) to the walls, which reduced the tunnel area, accelerated the flow to supersonic Mach numbers, and thereby prevented diffuser noise from propagating upstream. The bumps themselves, however, produce a perturbation to the uniform flow forward of their location which could adversely affect the test-section flow quality. The magnitude and extent of this

perturbation must therefore be known to insure proper positioning of the bumps in the tunnel. The rearward placement of the bumps is limited by the wall angles required on the back side of the bump to fair back into the tunnel diffuser section. If the wall angles behind the bump are too large, the boundary layer may separate in this region, which could create additional problems in the wind tunnel. Forward placement of the bumps is limited by the requirement for uniform flow at the model location. From these considerations, a location at the rear of the test section is the most desirable.

An inviscid analytical study was therefore conducted to determine the upstream influence of choke bumps for a Mach number range of 0.6 to 0.9. This study was made by using a computer program which is based on the stream-tube curvature method (refs. 3 and 4). This program is able to calculate the mixed subsonic-supersonic internal flows encountered in this problem. The geometry of the choke bump was systematically varied to examine the effect of shape on the disturbance produced.

SYMBOLS

A/A^*	tunnel area divided by throat area
C	wall curvature at the tunnel throat, 1/meters
H	tunnel height (or diameter) at the entrance, meters
h	choke bump height, meters
l	choke bump length, meters
M	local Mach number
M_{nom}	nominal free-stream Mach number
M_∞	actual free-stream Mach number
ΔM	$= M - M_\infty$
$\Delta\dot{m}$	mass-flow deficit, $1 - \frac{\text{Actual mass-flow rate}}{\text{Ideal mass-flow rate}}$
V/a^*	local velocity divided by speed of sound at $M = 1$
x	streamwise coordinate, origin at tunnel throat, meters
y	coordinate normal to tunnel center line, origin at center line, meters
y_t	tunnel half-height (or radius) at throat, meters

Subscripts:

℄	value at tunnel center line
w	value at tunnel wall

APPROACH

The computer program used in this study was the stream-tube curvature program, which is described in detail in references 3 and 4. It was chosen mainly because of its ability to handle mixed subsonic-supersonic flow inside of two-dimensional and axisymmetric ducts of arbitrary shape. The program at times encounters some difficulty in regions where the velocity is very close to the speed of sound, but this difficulty seems to have little effect on the regions of interest upstream of the throat.

This study was conducted by using only the inviscid calculations from the program. Although it is recognized that viscous effects may become important in some of the cases, some difficulties were encountered in applying the boundary-layer option in the program and in trying to define the levels of perturbation to the free stream. It is believed that the inviscid results should give a good indication of the extent of the disturbances in most of the cases.

The program generates a calculation grid that is approximately aligned along and normal to the streamlines for the given flow. It then moves the grid points to adjust the area, and therefore the velocity, for each stream tube while maintaining a given total mass-flow rate. These velocities must also match the cross-stream velocity gradients imposed by the curvature of the streamlines. The final grid in a converged run should, therefore, fairly accurately represent the actual streamline pattern for the flow. This alignment allows the program to calculate transonic flows fairly easily since the cross-derivative terms are eliminated from the equations of motion. An example of a final calculation grid is shown in figure 1. Note that the mesh spacing is smaller in the region of the throat, where the velocity gradients are higher. Computer run times averaged about 150 CPU seconds on the Control Data CYBER 175 computer system.

Two important program options that were utilized for the runs in this study were the choice of subsonic or supersonic flow downstream of the throat created by the choke bumps and the automatic adjustment of the total mass-flow rate to match the mass-flow rate required for choking the tunnel. The first option allows the user to specify that, if the flow chokes, the Mach numbers downstream of the throat will increase for increasing stream-tube area. This option will cause the supersonic region to extend across the entire tunnel, which is the desired situation for the prevention of the disturbances from traveling upstream through the throat. This is also physically what will happen in a tunnel when the pressure downstream of the throat is sufficiently low.

The second option, which allows an automatic adjustment of the mass-flow rate to match the maximum flow rate, was found to be very useful. The bump

heights required to choke the flow at the given free-stream Mach numbers were calculated using one-dimensional isentropic relations. Using these relations implies a uniform Mach number of 1.0 across the throat and the maximum mass-flow rate for the given stagnation conditions. The actual flow is two-dimensional, though, with a supersonic Mach number at the wall of the throat and a subsonic Mach number at the center line. This means that the actual mass-flow rate through the throat will be somewhat less than the ideal maximum. The program calculates the area required by the actual mass flow, then adjusts the mass flow if this area does not match the physical area of the throat. This feature eliminated the need for multiple runs using manual adjustment of the flow rate and, in general, aided in program convergence.

Since the mass-flow rate was always reduced below the input ideal level value, the actual free-stream Mach number was also less than the nominal value. As seen in figure 2, this reduction was fairly small except for a few cases at $M_{nom} = 0.9$, where some difficulties with program convergence were experienced. The cases that have a large deviation from the nominal Mach number (in particular, the axisymmetric circular-arc bump with $l/h = 10$ at $M_{nom} = 0.9$) should not be used for comparison purposes but may be useful in indicating approximate regions of upstream disturbances. The cases will generally be referred to by their nominal free-stream Mach numbers.

The basic computational model was a constant-area tunnel with a bump added to the walls. The bump height was calculated using isentropic relations so that the flow was choked in an equivalent one-dimensional channel at the nominal Mach number. This calculation resulted in eight different bump heights, one for each nominal Mach number that was run for the two-dimensional and axisymmetric bump configurations. Because of the symmetry involved in the problem, the flow field was determined only from the center line of the tunnel to the wall. A sufficient length of tunnel upstream of the choke bump was specified so that the uniform conditions across the entrance of the tunnel were maintained for at least one more grid station. The tunnel was continued downstream of the throat in such a manner that the flow remained supersonic and returned to a fairly uniform state.

Two basic choke bump shapes were examined in this study: a fifth-degree polynominal curve and a circular arc. These shapes were chosen because they are similar to choke bumps that have been or will be used in wind-tunnel tests. The polynomial curve was generated so that it had zero slope and zero curvature at the beginning, thereby it would fair smoothly into the wall. This curve also had zero curvature as well as zero slope at the tunnel throat. The maximum angle for the polynomial occurred midway between the beginning of the curve and the tunnel throat. The circular-arc curve had constant curvature from the beginning of the bump to the tunnel throat and had its maximum angle at the beginning where it intersected the tunnel wall to form a stagnation point. Both curves continued in a symmetric manner for a short distance beyond the throat then were faired back into the tunnel wall at a distance of 1 tunnel height past the minimum area point. This fairing was done by the program and simplified the calculations by eliminating the rear stagnation point for the circular arc and the higher curvature in that region for the polynomial curve. Since the fairing was downstream of the throat in the supersonic region, it should have no effect on the flow disturbances upstream of the choke bump.

Each of the two basic curves was run at values of l/h of 10 and 20 where l is the distance from the beginning of the choke bump to the tunnel throat and h is the height of the bump from the tunnel wall. (See fig. 3.) The shorter chokes had angles about twice as large and curvatures about four times as large as the longer chokes. The maximum angles for the two circular-arc chokes were 11.42° and 5.77°, and the maximum angles for the two polynomial curves were 10.62° and 5.36°. Each configuration was run as an axisymmetric as well as a two-dimensional computational model. This should give some indication of the effects of putting choke bumps on all the tunnel walls as well as just two walls.

For this study, l/h was used as a variable so that the shapes would be similar at a given l/h for different Mach numbers. If a variable choke bump that was to be effective over a range of Mach numbers was installed in a tunnel, it would most likely have a fixed value of l. The parameter l/h would then no longer be fixed for different Mach numbers but would vary with the value of h required to choke the tunnel.

RESULTS AND DISCUSSION

As previously stated, the stream-tube curvature program was selected for use because of its ability to handle transonic internal flows. Some transonic cases were included as examples in reference 3, but none of these were similar to the configurations of the present study. It was therefore decided to run some test cases to check the program results against an exact solution for flow through a choked passage. Oswatitsch and Rothstein (ref. 5) calculated the velocities in a hyperbolic convergent-divergent nozzle with supersonic flow downstream of the throat. Their results include a "final solution" for a two-dimensional nozzle and a first approximation for the axisymmetric case. The cases having a wall curvature at the throat of 0.2 times the throat half-height (i.e., $Cy_t = 0.2$) were selected for comparison. As shown in figure 4, the velocity profiles calculated by the stream-tube curvature program are in excellent agreement with the exact calculations for both the two-dimensional and axisymmetric nozzles. These results indicate that the stream-tube curvature program is adequate for the study of a tunnel with choke bumps.

Tunnel ΔM Contours

The variation of Mach number in the tunnel for the various choke bump configurations is illustrated in figures 5 through 8. The contours are shown for several values of ΔM, defined as $\Delta M = M - M_{\infty}$. Using ΔM instead of M to generate the contours helped reduce the differences between runs due to the variation in M_{∞}. A comparison was made of two runs having the same nominal Mach number but converging to slightly different actual free-stream Mach numbers. (A small change in the initial input of mass-flow rate caused the program to converge along a slightly different path.) This comparison showed that the ΔM-contour patterns for the two runs were the same to the accuracy of the plotter in the regions of interest. Differences were noted in the vicinity of the sonic line where the flow is very sensitive to changes in mass flow. Since the shape and location of the sonic line did vary, it is not included in the plots.

The general appearance of the contour pattern was similar for all the cases that were run (figs. 5 through 8). All runs had the Mach numbers near the wall dropping below M_∞ as the flow approached the choke bump. The minimum Mach number was reached at the stagnation point for the circular-arc bump and in the vicinity of the maximum negative curvature for the polynomial curve. The flow then accelerated up to and beyond the free-stream Mach number as it went further downstream. The displacement of the streamlines towards the center line due to the bump caused the Mach numbers in the center of the tunnel to be greater than the free-stream Mach number. For the smaller contour values on the two-dimensional plots, the contours for positive ΔM intersected the center line about the same distance upstream as the contours for negative ΔM of the same magnitude intersected the wall ahead of the choke bump. On the plots for the axisymmetric cases, the contours for positive ΔM went farther upstream than did the contours for negative ΔM. In most cases, the contour for $\Delta M = 0.1$ was approximately straight across the tunnel. This line was not well defined in some of the higher Mach number runs, and it is believed that program convergence problems contributed to this condition. Therefore, the contours presented use the farthest upstream occurrences of the $\Delta M = 0.1$ values.

Center-Line Perturbation Levels

Generally, the farthest upstream effect of a given perturbation occurred on the tunnel center line. Since the center line is also the approximate location for a model in most wind-tunnel tests, the upstream distance along this line for the given values of ΔM are compared for the various configurations. Figures 9 and 10 show ΔM along the center line as a function of x/H, the distance upstream of the throat nondimensionalized by the tunnel height (tunnel diameter for the axisymmetric cases). Figure 9 gives results for the two-dimensional cases, whereas figure 10 gives results for the axisymmetric cases, with each plot representing a given nominal Mach number.

As seen in figure 9(a), for a given length-to-height ratio, the polynomial-curve choke bump had a smaller perturbation level at a given distance upstream than did the circular-arc choke bump. This probably resulted from the smaller wall angles and reduced thicknesses which occurred over the forward portion of the polynomial curve bump. This difference in geometry between the two bump shapes would cause the streamlines to be displaced less towards the center line at a given distance upstream, resulting in lower center-line velocities, for the polynomial-curve case. The advantage of the polynomial curve over the circular arc was less at the lower length-to-height ratio. Changing l/h from 20 to 10 for a given basic shape also indicated a potential benefit. Even though this change increased the thicknesses and wall angles for the front of the bump, possibly increasing the perturbation generated, the locations of these points were shifted much farther downstream and more than compensated for any such effect. All these trends were also true for $M_{nom} = 0.7$ and 0.8, as shown in figures 9(b) and 9(c), respectively, although the stated benefits decreased with increasing Mach number. Figure 9(d) shows that, at a nominal Mach number of 0.9, none of the configurations was significantly better than any other. Some reversals in the curves are apparent for the higher values of ΔM at this Mach number; this is believed to be mainly the result of convergence problems in the program.

These problems may not allow a good comparison of configurations but a general idea of the upstream distance for various perturbation levels at this Mach number can be obtained.

Viscous effects tend to reduce the advantages mentioned. The boundary layer effectively forms a fillet at the leading edge of the circular arc, making it more like the polynomial curve. Also, as l/h is reduced and angles on the bumps increase, the boundary layer in front of the bump will tend to thicken, increasing the effective length of the bump, and therefore, l/h.

It can be seen in figure 10 that the trends observed in the two-dimensional cases also held true for the axisymmetric runs. The magnitude of the differences between configurations was reduced by going to the axisymmetric choke bumps. Also, for the same basic shape and length-to-height ratio, the axisymmetric configurations generally produced a smaller disturbance than the two-dimensional cases at the same upstream distance. This is due mainly to the fact that a smaller bump height is required to reach a given A/A^* for the axisymmetric case compared to the two-dimensional case. For a given length-to-height ratio, a shorter length bump will therefore result. The $M_{nom} = 0.9$ cases, plotted in figure 10, show almost no advantage of one configuration over the other, as was true for the corresponding two-dimensional runs.

Region of Significant Disturbance Levels

A variation in the free-stream Mach number of 0.001 should have no significant effect on the results of wind-tunnel tests and is about the accuracy of the measured Mach number for many tunnels. This value of ΔM will therefore be used as a basis for some further comparisons between configurations. Figure 11 shows the upstream distance (nondimensionalized by tunnel height) of the intersection of the contour for $\Delta M = 0.001$ with the tunnel center line for different configurations and Mach numbers. For Mach numbers up to $M_{nom} = 0.8$, the short polynomial-curve choke bump had the shortest upstream disturbance distance, followed by the short circular arc, the long polynomial curve, and finally the long circular arc. Above $M_{nom} = 0.8$, the lines are dashed in figure 11 to indicate that comparisons between configurations may not be valid because of program convergence problems encountered in some of the $M_{nom} = 0.9$ cases. For the $M_{nom} = 0.6$ to 0.8 range, using a short polynomial-curve choke bump would reduce the unacceptable perturbation region to about two-thirds of that generated by the long circular-arc choke bump at any given Mach number. A comparison of figure 11(a) with figure 11(b) shows that additional reductions may be obtained by using the axisymmetric configuration. The unacceptable region for the long two-dimensional circular-arc cases was more than twice as long, on the average, as the region for the short axisymmetric polynomial-curve cases.

Some insight into the reason for these advantages may be gained from the contour plots (figs. 5 through 8). If the upstream distance to the intersection of the $\Delta M = 0.001$ contour with the tunnel center line is measured from the intersection of the $\Delta M = 0.001$ contour with the tunnel wall instead of from the throat, these distances appear similar for the different configurations. Figure 12, which plots $(x/H|_{\Delta M=0.001})_{\ell} - (x/H|_{\Delta M=0.001})_{w}$ against M_{nom}

for all the configurations, confirms this. The distance values all fall within a fairly small band at any given Mach number, and even between Mach numbers, the variation is not large; this would indicate that the primary way of reducing the upstream disturbance distance is to move the point at which the Mach number of the wall reaccelerates to about the free-stream value as close to the throat as possible.

Flow Parameter Estimation

As noted before, there may be small differences between runs at the same nominal Mach number because of the program converging to slightly different actual free-stream Mach numbers. The variation of the actual mass-flow rate from the ideal mass-flow rate generally increased with increasing maximum curvature for the configurations. In an attempt to estimate the correct mass flow and aid in program convergence, the parameter Cy_t (the curvature at the throat times the tunnel half-height at the throat) was plotted against the mass-flow deficit given by $\dot{\Delta m} = 1 - \frac{\text{Actual mass-flow rate}}{\text{Ideal mass-flow rate}}$. This is shown in figure 13(a) for the circular arc. Since the curvature at the throat was always zero for the polynomial curve, the maximum curvature was used instead of the throat curvature, with the results shown in figure 13(b).

For values of Cy_t up to about 0.2, a good correlation between mass-flow deficit and Cy_t is found for the circular-arc cases. Below $Cy_t = 0.2$, the mass-flow deficit is closely approximated by $0.021(Cy_t)^{1.92}$. For value of Cy_t greater than 0.2, this approximation gave a larger mass-flow deficit than actually occurred in the computer results. It is interesting to note that when the results from the two hyperbolic nozzle test cases shown in figure 4 were plotted in figure 13(a), they fell very close to the circular-arc values. No similar correlation was evident in figure 13(b) for the polynomial curve. This result might be expected since the maximum curvature occurred at a fairly good distance from the throat for many configurations.

An examination of the throat Mach numbers for the circular-arc cases revealed that, for values of Cy_t up to about 0.2, the throat Mach number at the wall and at the center line also correlated with Cy_t. Figure 14 shows this correlation, with the solid line representing the estimates for the two-dimensional runs, and the dashed line approximating the axisymmetric runs. The two-dimensional results were approximated by using $M_w = 1 + 0.4Cy_t - 0.1(Cy_t)^2$ and $M_{\ell} = 1 - 0.2Cy_t + 0.05(Cy_t)^2$, and the axisymmetric results were approximated by using $M_w = 1 + 0.3Cy_t - 0.075(Cy_t)^2$ and $M_{\ell} = 1 - 0.3Cy_t + 0.2(Cy_t)^2$. Once again, the hyperbolic nozzle results were also fairly well predicted by using the approximations for the circular arc.

It was found that, after some algebraic manipulation and simplification, the exact solutions formulated by Kliegel and Levine (ref. 6) for flow through axisymmetric nozzles and by Hall (ref. 7) for flow through two-dimensional nozzles produced similar correlations for the given flow parameters with the geometry parameter Cy_t (note that Cy_t is given as $1/R$ in refs. 6 and 7). For the axisymmetric nozzle, the throat Mach number would be approximated by

$M_{\ell} = 1 - 0.3Cy_t + 0.296(Cy_t)^2$ and $M_w = 1 + 0.3Cy_t - 0.144(Cy_t)^2$, and the mass-flow deficit would by given by $\Delta\dot{m} = 0.0250(Cy_t)^2 - 0.0335(Cy_t)^3$. For the two-dimensional nozzle, the throat Mach numbers would be approximated by $M_{\ell} = 1 - 0.2Cy_t + 0.140\ (Cy_t)^2$ and $M_w = 1 + 0.4Cy_t - 0.154(Cy_t)^2$, with the mass-flow deficit estimated by $\Delta\dot{m} = 0.0267(Cy_t)^2 - 0.0300(Cy_t)^3$. For $Cy_t \leq 0.2$, these approximations give results that are very similar to the ones given by the empirical approximations; this adds further support to the results of this study.

SUMMARY OF RESULTS

An inviscid study was made by using a computer program based on the stream-tube curvature method to determine the upstream flow perturbation due to placing choke bumps in a tunnel. The computer runs were made for a free-stream Mach number range of 0.6 to 0.9, with both two-dimensional and axisymmetric tunnel models. Several choke bump shapes were analyzed to determine any effects due to geometry on the magnitude of the disturbance generated. The main results of this study are summarized as follows:

1. For length-to-height ratio (ℓ/h) and bump shape fixed, the distance upstream of the throat at which a significant perturbation (nominal minus actual free-stream Mach number ΔM of 0.001) Mach number would occur decreased as the nominal free-stream Mach number increased.

2. The axisymmetric choke configurations generally had a smaller upstream disturbance distance than did the corresponding two-dimensional configurations.

3. The $\ell/h = 10$ configurations generally had a smaller upstream disturbance distance than did the corresponding $\ell/h = 20$ configurations.

4. The polynomial-curve configurations generally had a smaller upstream disturbance distance than did the corresponding circular-arc configurations.

5. The primary means of reducing the upstream disturbance distance appeared to be to move closer to the throat the point on the wall at which the Mach number reaccelerates to about the free-stream value.

6. For values of the parameter Cy_t (curvature at throat times tunnel half-height at throat) up to about 0.2, the mass-flow deficit and the Mach numbers at the wall and center line of the throat, could be approximated, for the circular-arc cases, as functions of Cy_t.

Finally, viscous effects, which were not included in this study, could be important for some of the cases and would probably tend to reduce some of the configuration advantages mentioned.

Langley Research Center
National Aeronautics and Space Administration
Hampton, VA 23665
July 15, 1981

REFERENCES

1. Pope, Alan; and Goin, Kennith L.: High-Speed Wind Tunnel Testing. Robert E. Krieger Pub. Co., 1978.

2. Brooks, Joseph D.; Stainback, P. Calvin; and Brooks, Cuyler W., Jr.: Additional Flow Quality Measurements in the Langley Research Center 8-Foot Transonic Pressure Tunnel. A Collection of Technical Papers - AIAA 11th Aerodynamic Testing Conference, Mar. 1980, pp. 138-145. (Available as AIAA-80-0434.)

3. Keith, J. S.; Ferguson, D. R.; Merkle, C. L.; Heck, P. H.; and Lahti, D. J.: Analytical Method for Predicting the Pressure Distribution About a Nacelle at Transonic Speeds. NASA CR-2217, 1973.

4. Ferguson, D. R.; and Keith, J. S.: Modification of the Streamtube Curvature Program. Volume I - Program Modifications and User's Manual. NASA CR-132705, 1975.

5. Oswatitsch, Kl.; and Rothstein, W.: Flow Pattern in a Converging-Diverging Nozzle. NACA TM 1215, 1949.

6. Kliegel, J. R.; and Levine, J. H.: Transonic Flow in Small Throat Radius of Curvature Nozzles. AIAA J., vol. 7, no. 7, July 1969, pp. 1375-1378.

7. Hall, I. M.: Transonic Flow in Two-Dimensional and Axially-Symmetric Nozzles. Q. J. Mech. & Appl. Math., vol. XV, pt. 4, Nov. 1962, pp. 487-508.

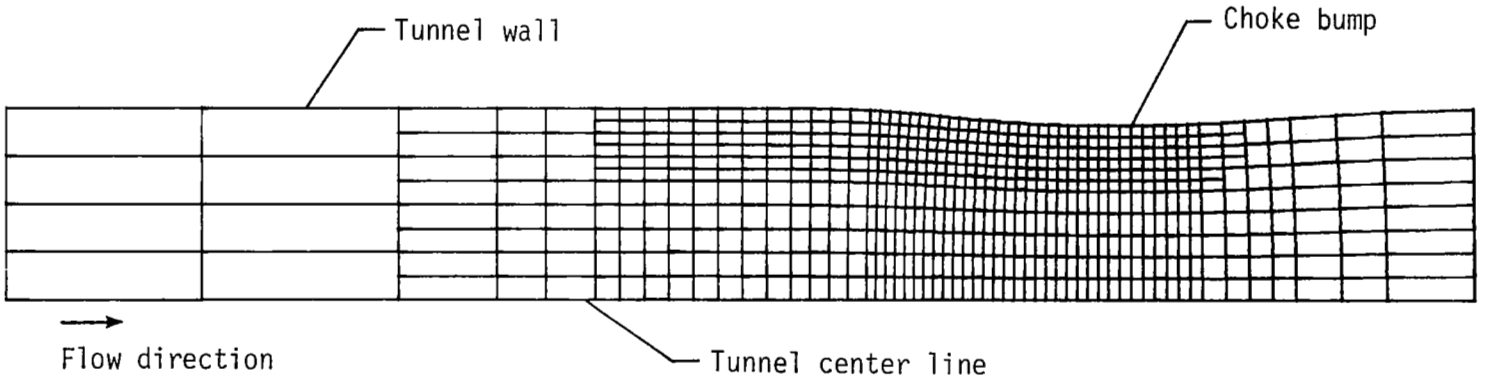

Figure 1.- Typical computational grid.

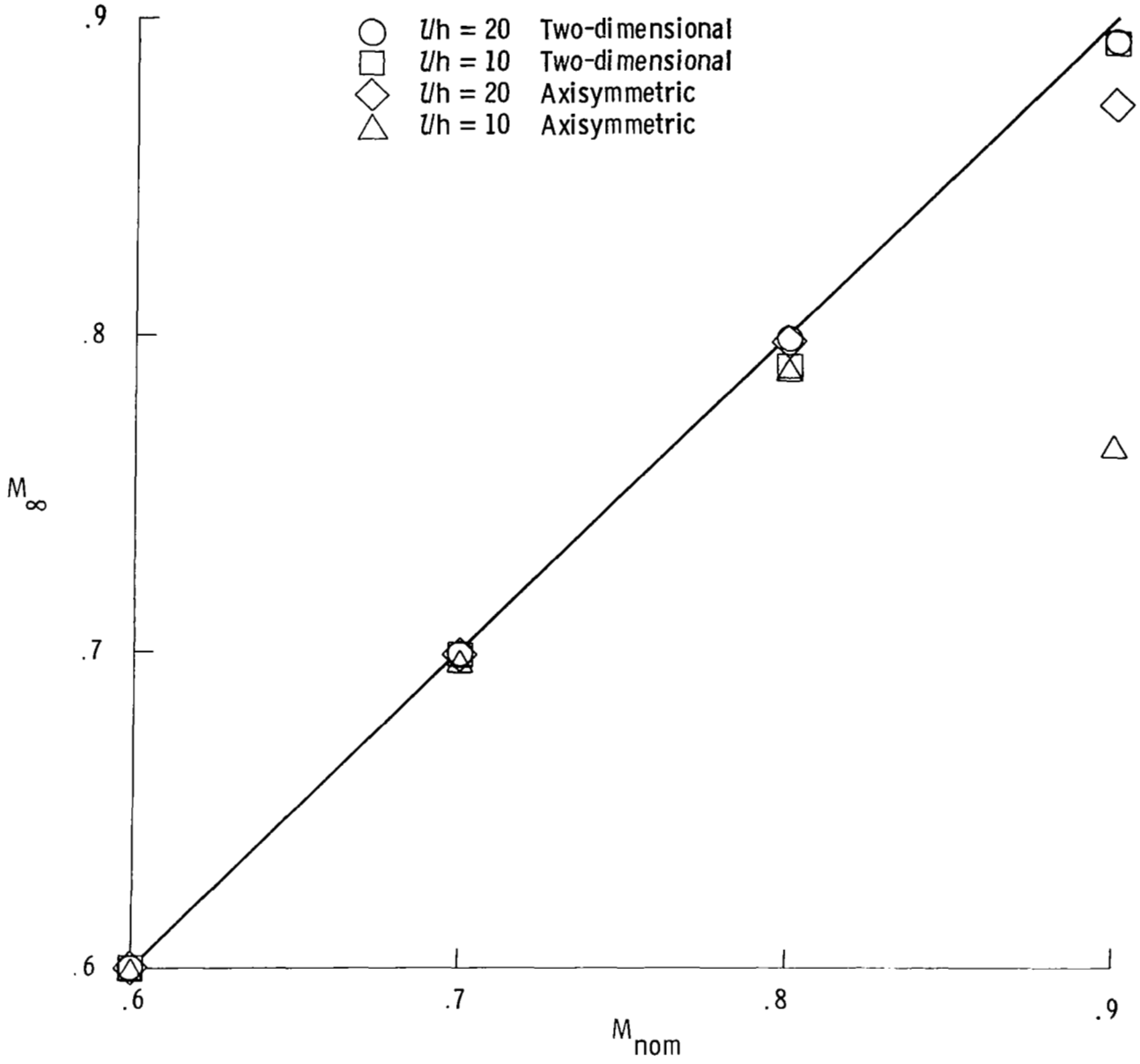

(a) Circular-arc choke bump cases.

Figure 2.- Comparison of actual and nominal free-stream Mach numbers.

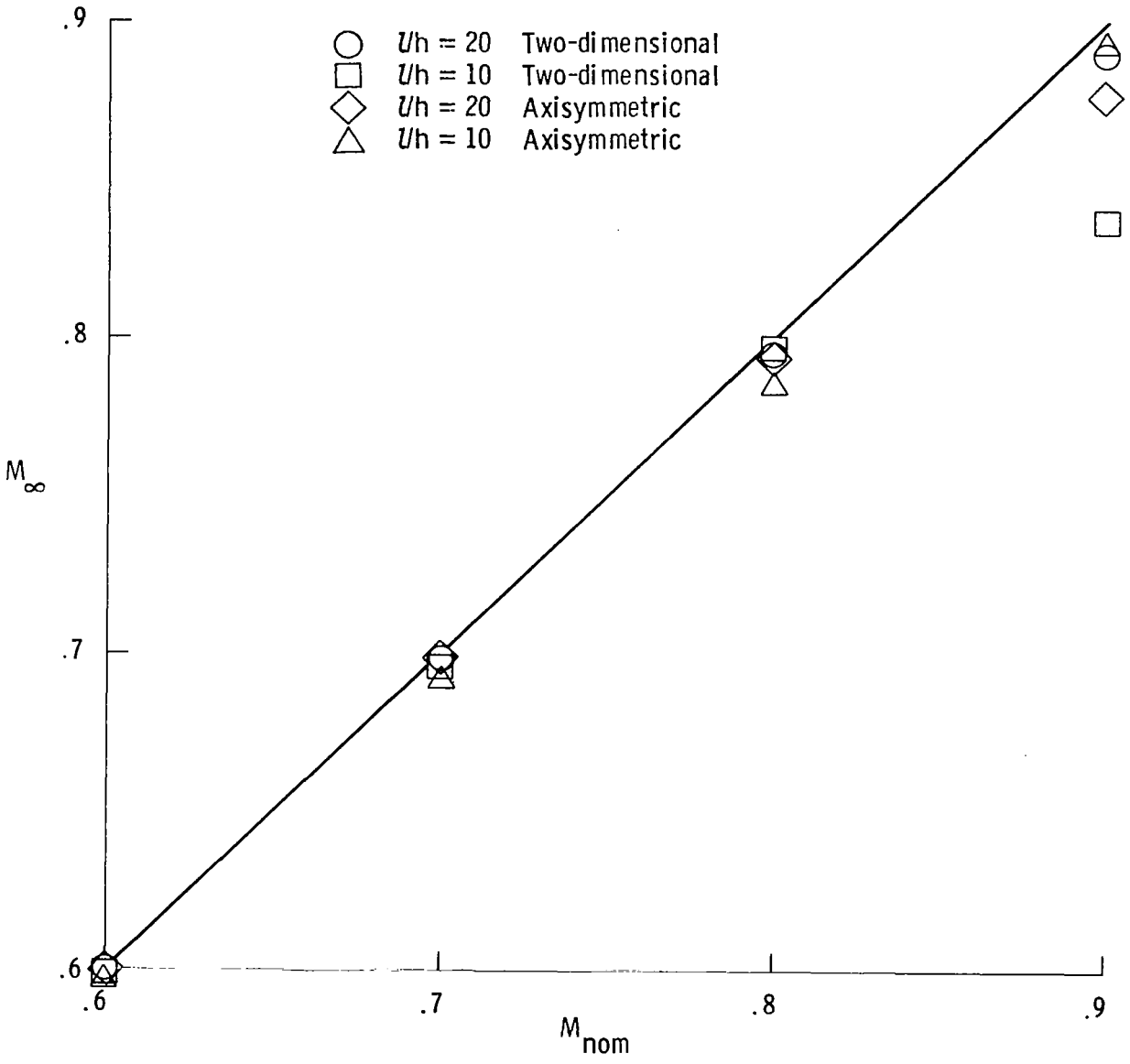

(b) Polynomial-curve choke bump cases.

Figure 2.- Concluded.

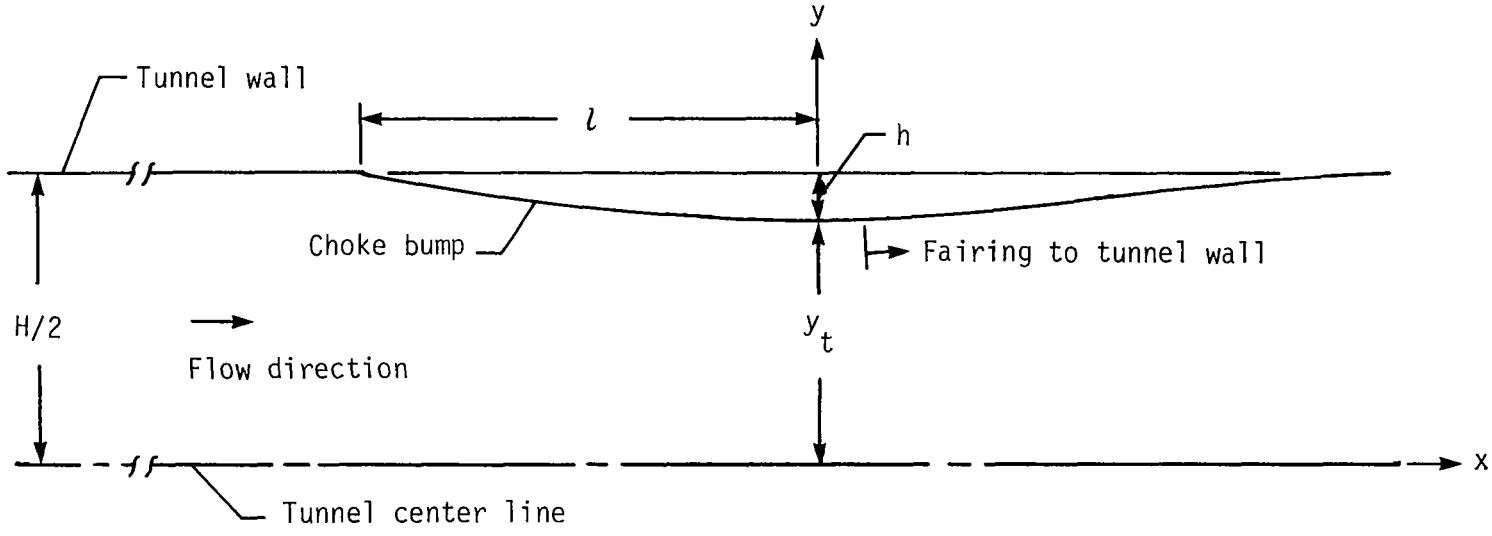

Figure 3.- Computer model geometry for choke bump in tunnel.

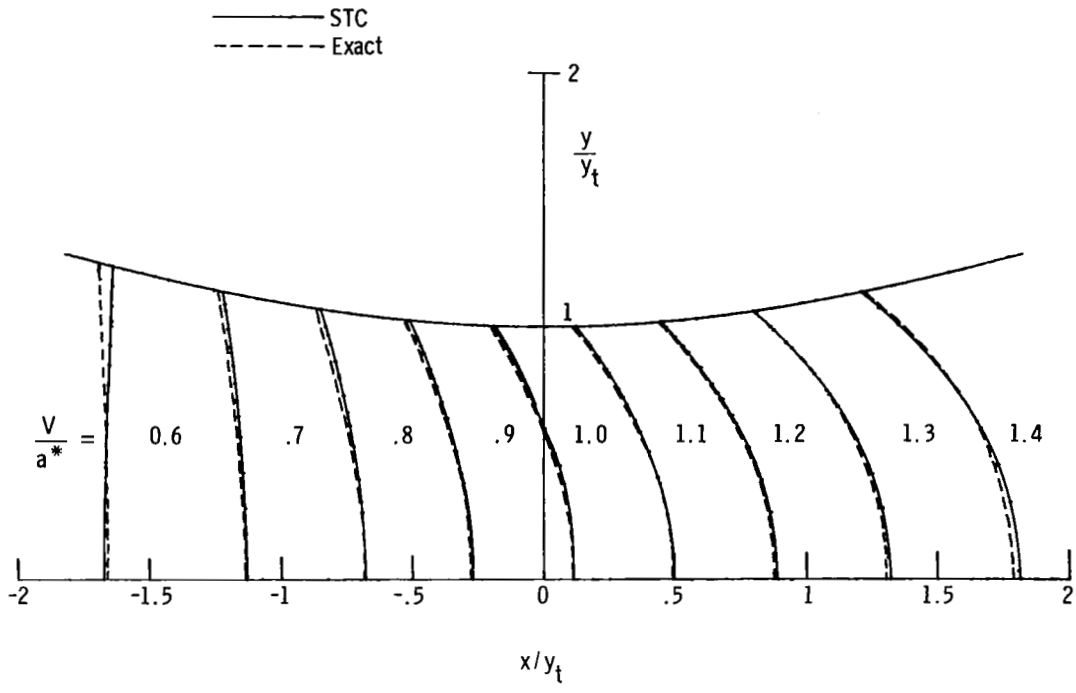

(a) Two-dimensional nozzle.

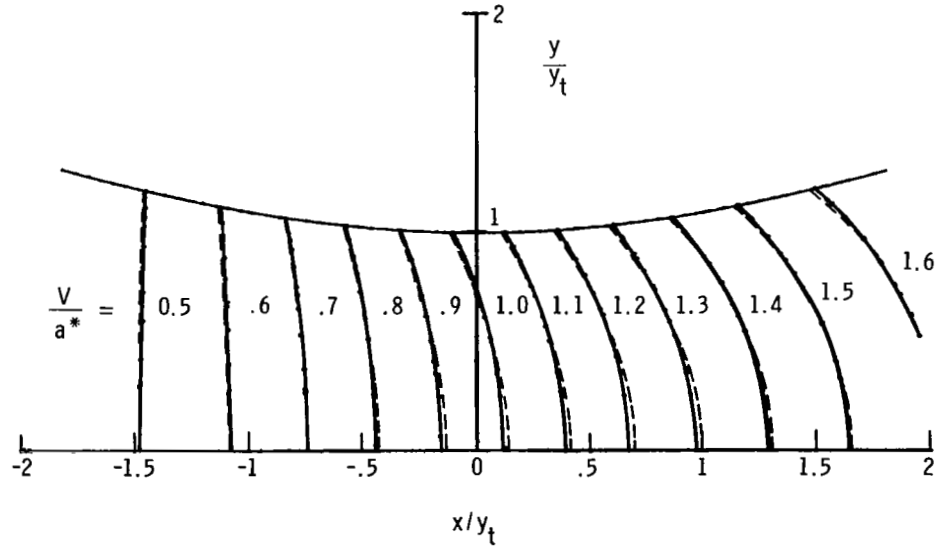

(b) Axisymmetric nozzle.

Figure 4.- Comparison of the stream-tube curvature (STC) program calculations for flow field in certain nozzles with exact solutions (ref. 5).

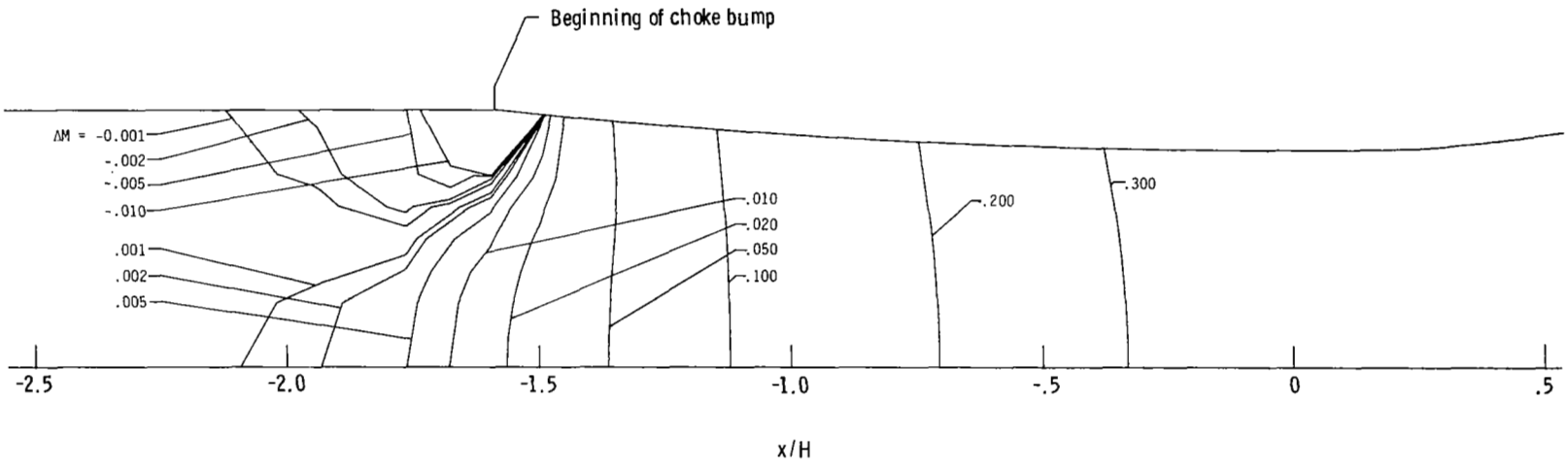

(a) $M_{nom} = 0.6; \quad l/h = 20.$

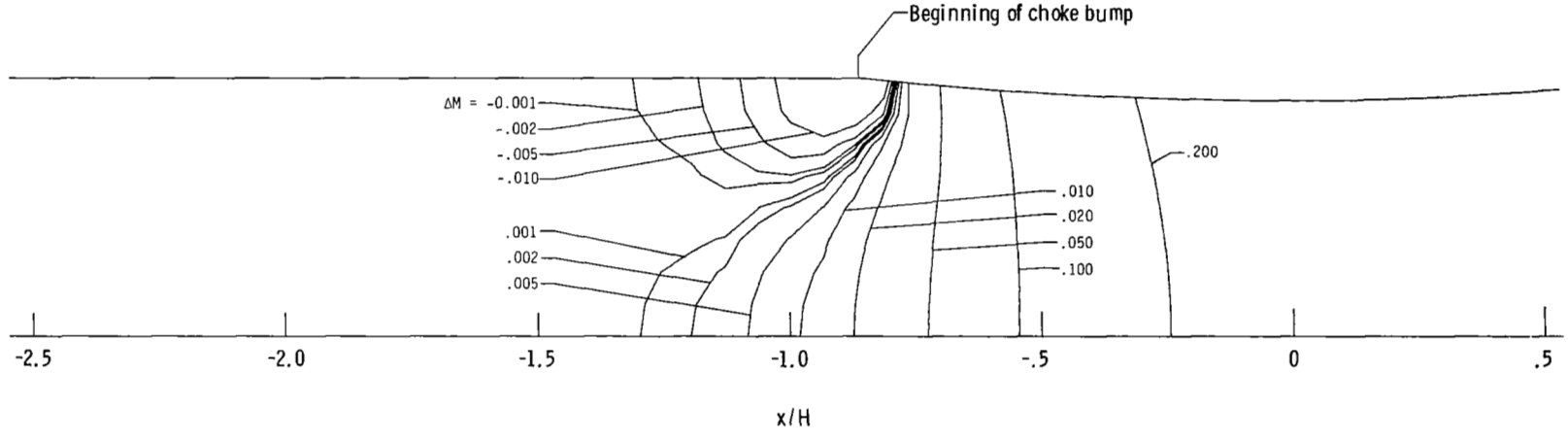

(b) $M_{nom} = 0.7; \quad l/h = 20.$

Figure 5.- Mach number variation in tunnel for two-dimensional circular-arc choke bump cases.

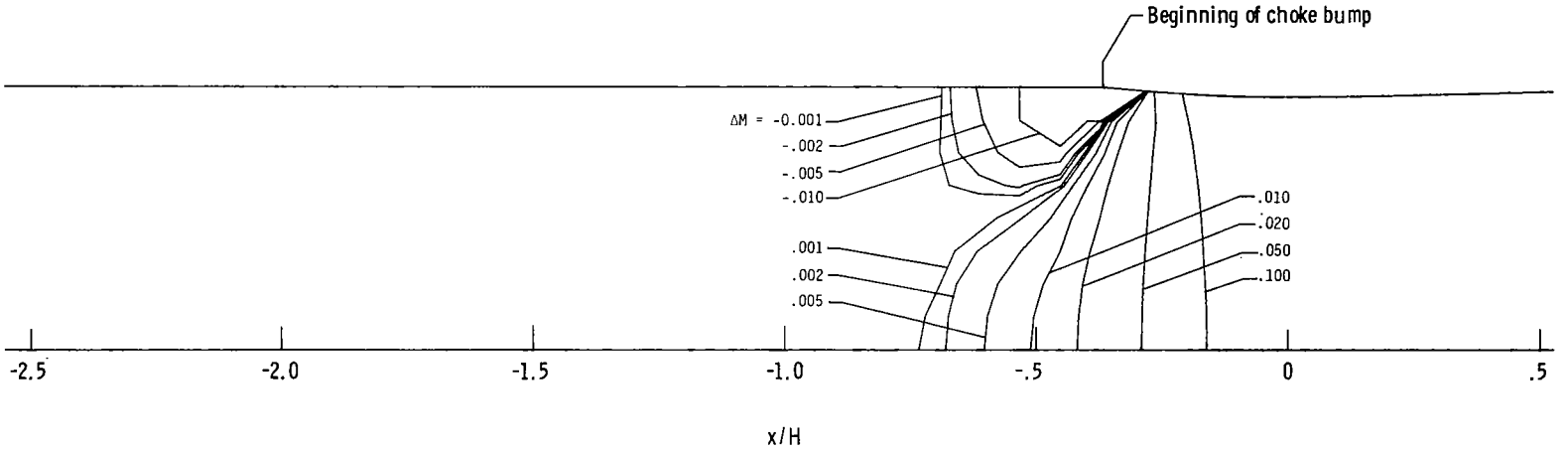

(c) $M_{nom} = 0.8$; $l/h = 20$.

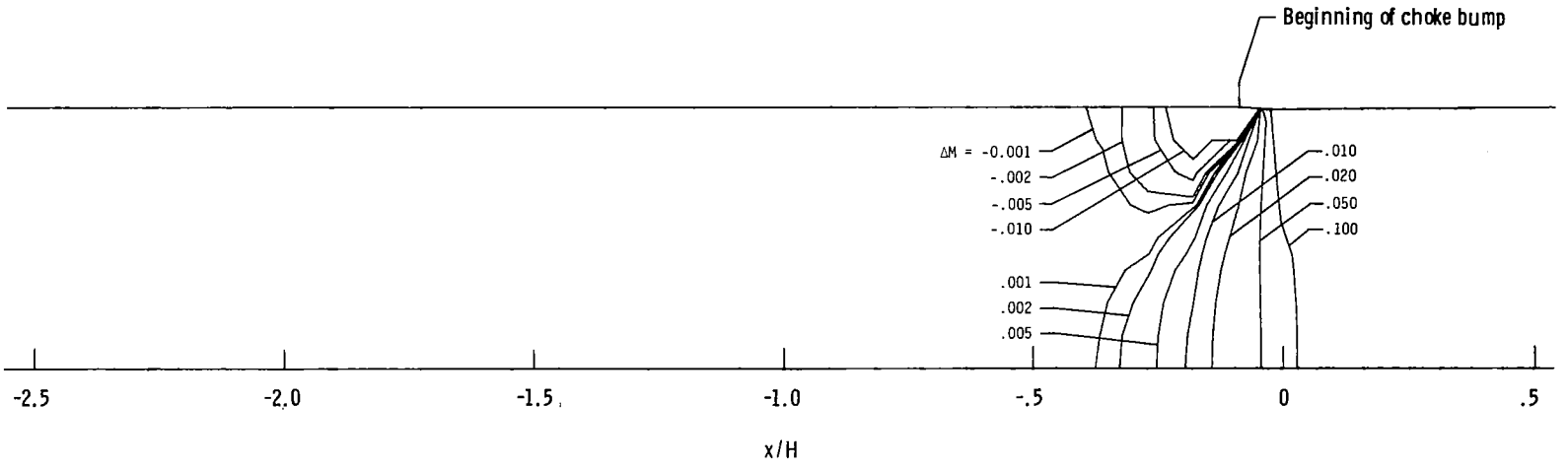

(d) $M_{nom} = 0.9$; $l/h = 20$.

Figure 5.- Continued.

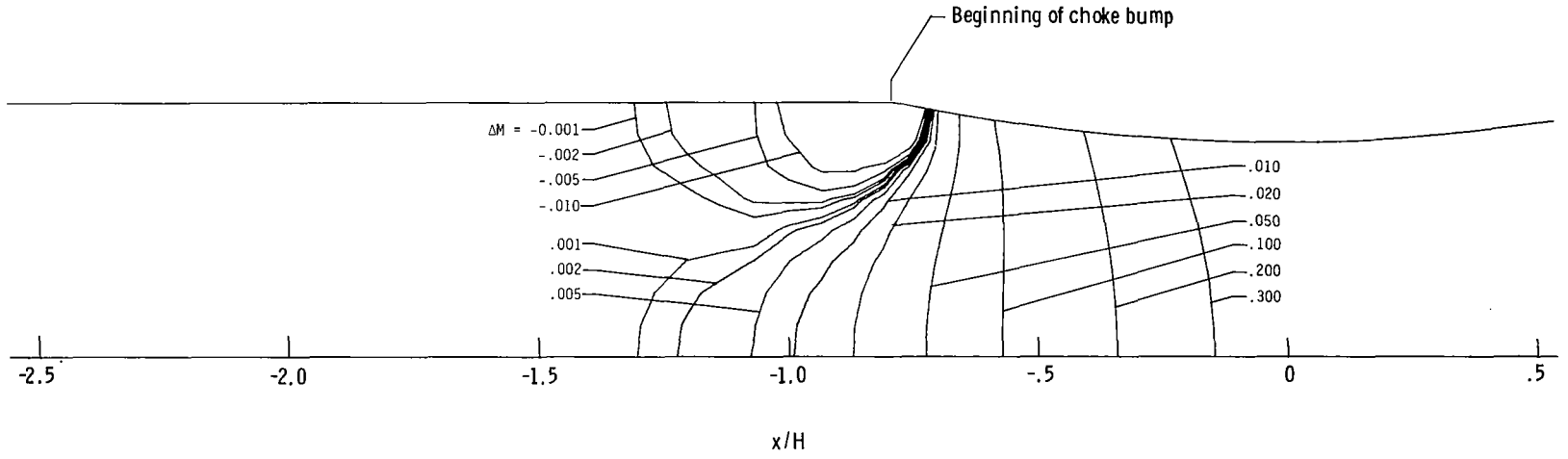

(e) $M_{nom} = 0.6$; $l/h = 10$.

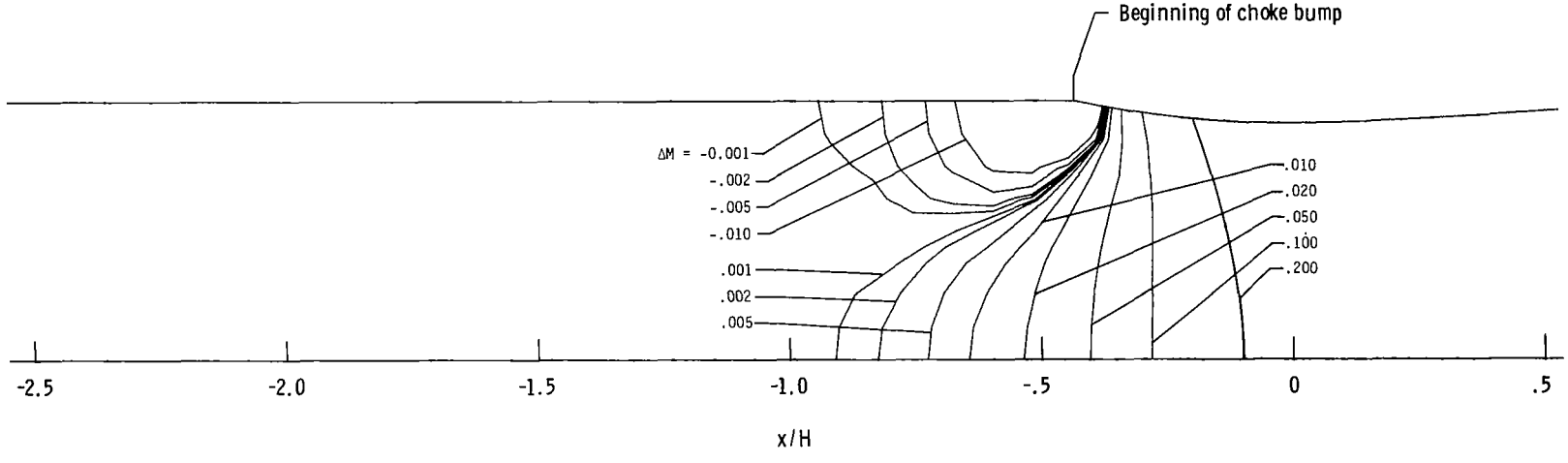

(f) $M_{nom} = 0.7$; $l/h = 10$.

Figure 5.- Continued.

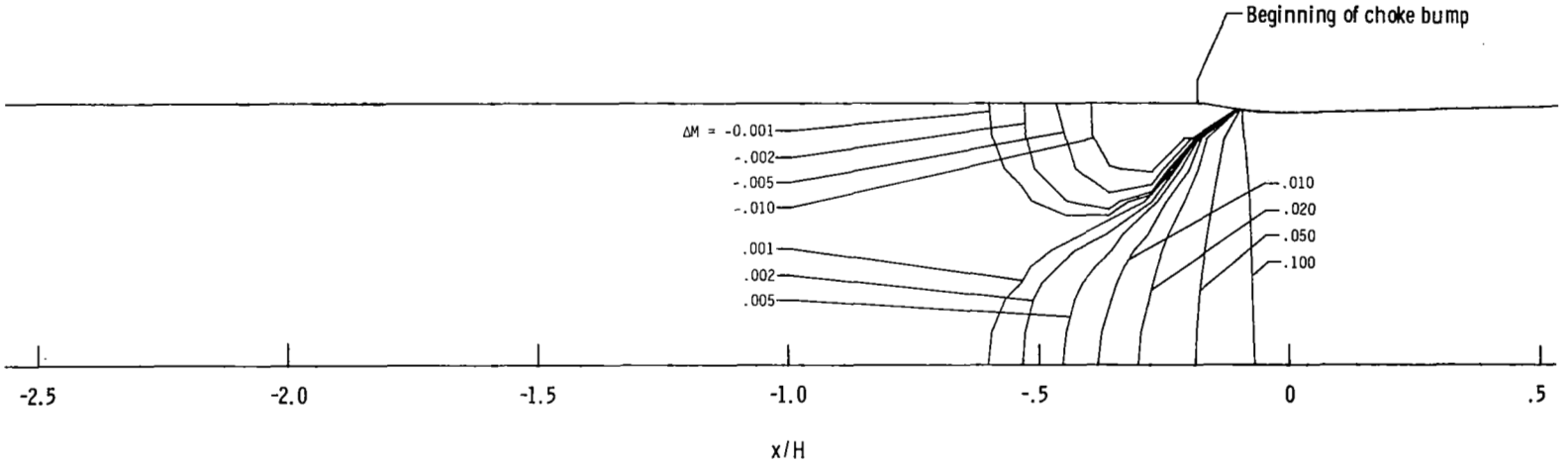

(g) $M_{nom} = 0.8$; $\ell/h = 10.$

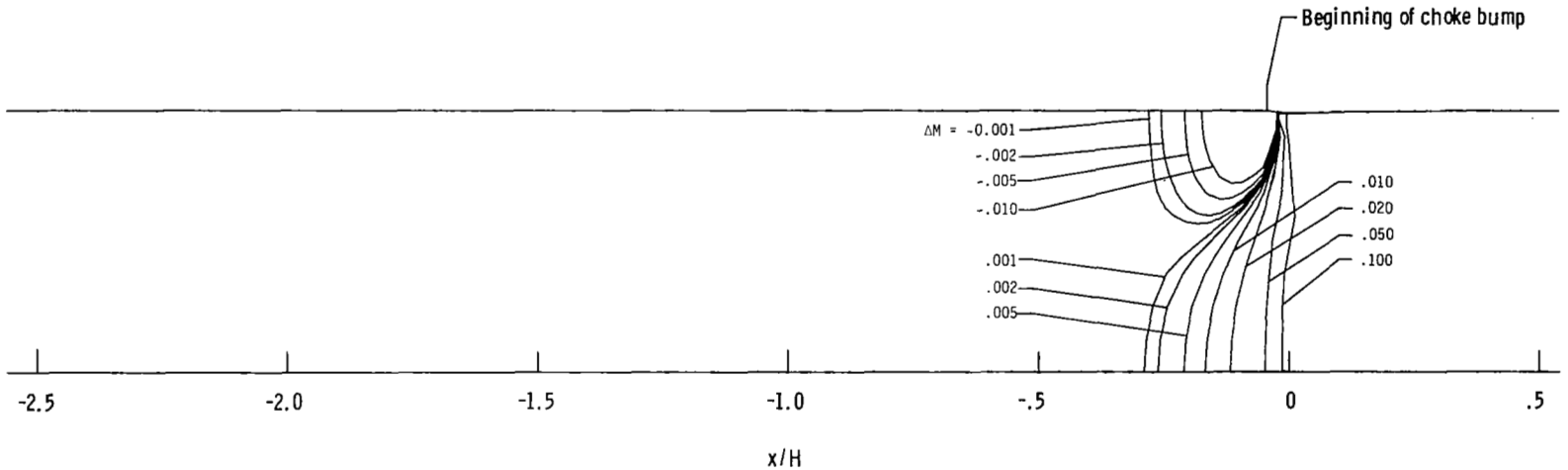

(h) $M_{nom} = 0.9$; $\ell/h = 10.$

Figure 5.- Concluded.

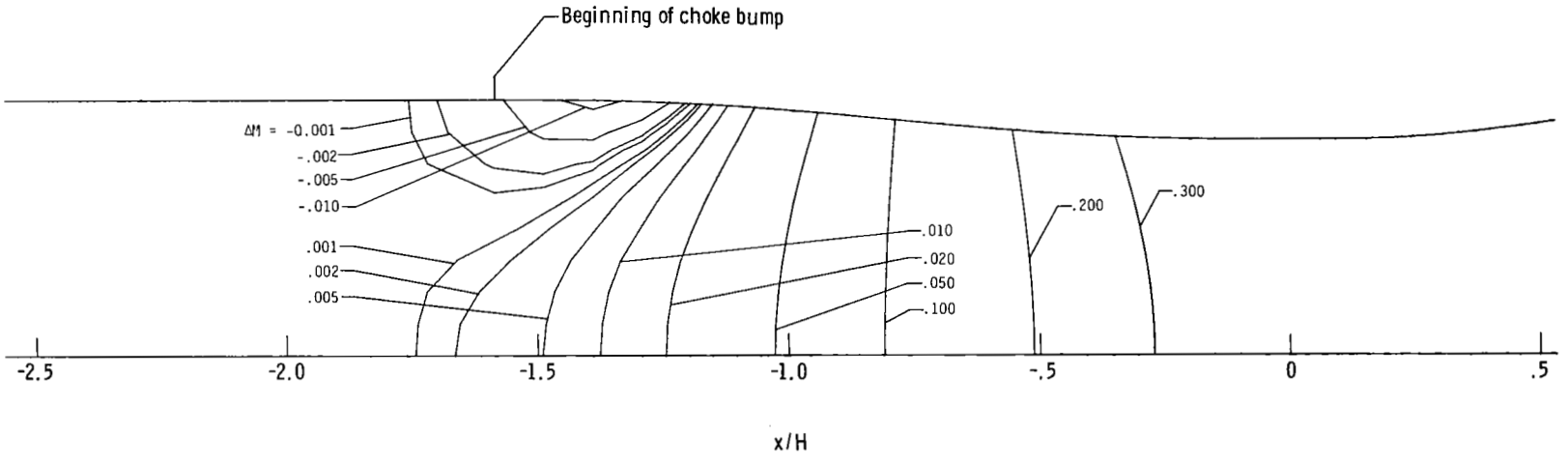

(a) $M_{nom} = 0.6$; $l/h = 20$.

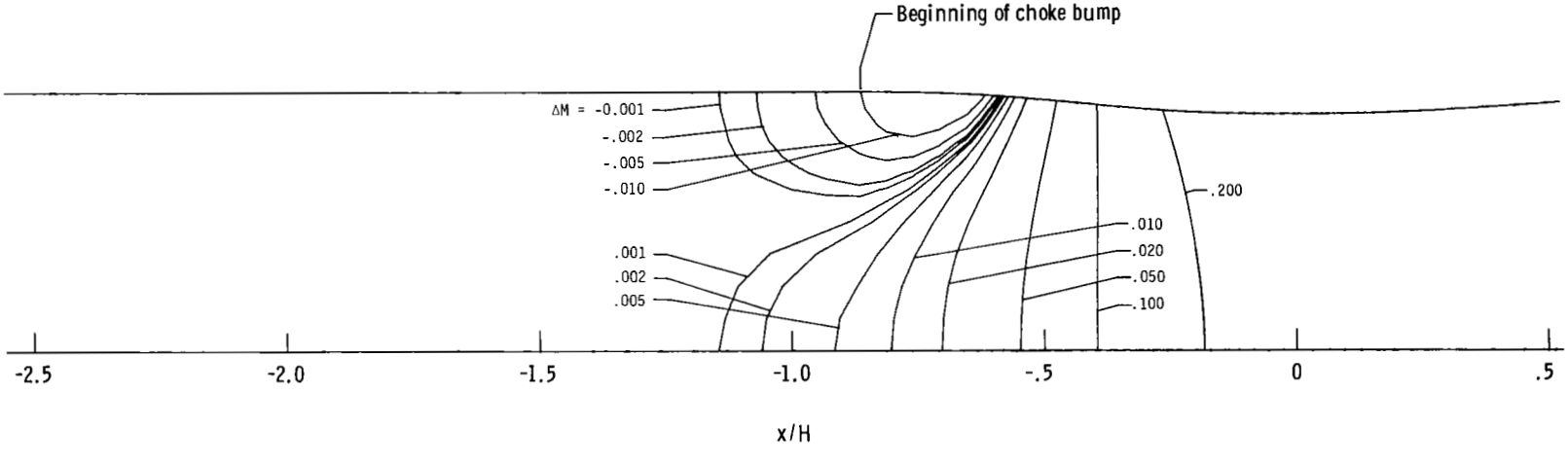

(b) $M_{nom} = 0.7$; $l/h = 20$.

Figure 6.- Mach number variation in tunnel for two-dimensional polynomial-curve choke bump cases.

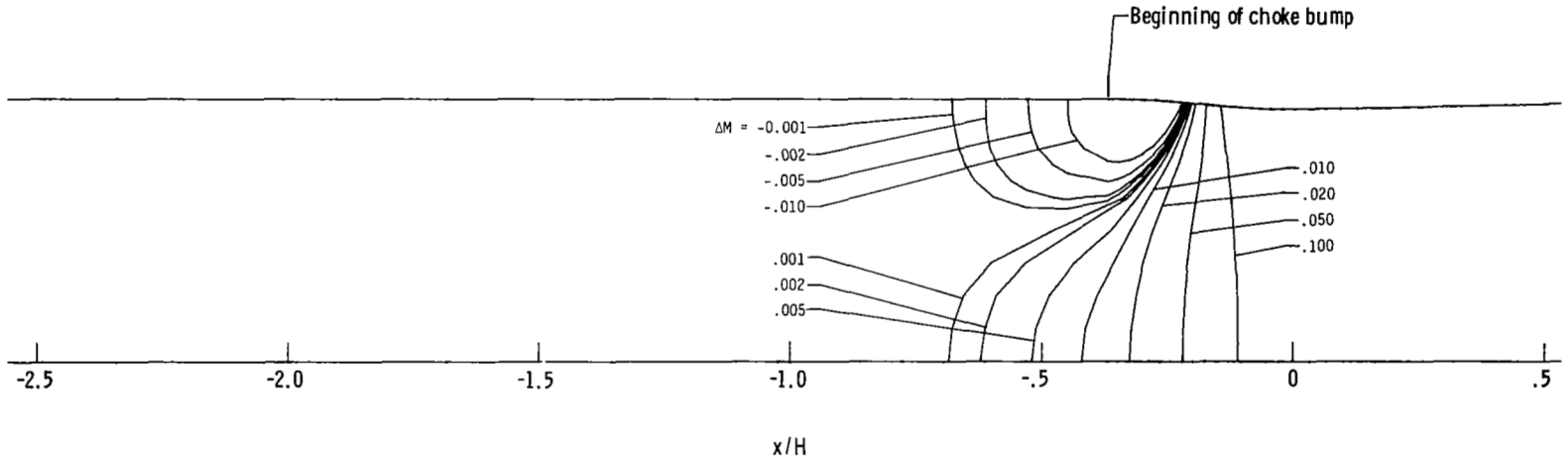

(c) $M_{nom} = 0.8$; $l/h = 20$.

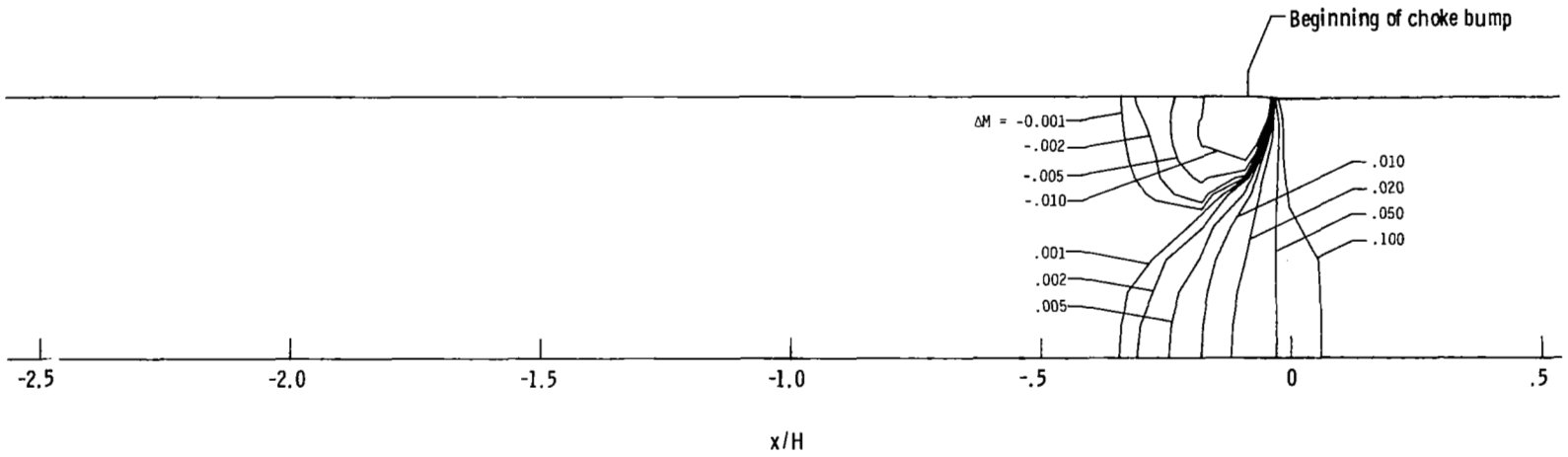

(d) $M_{nom} = 0.9$; $l/h = 20$.

Figure 6.- Continued.

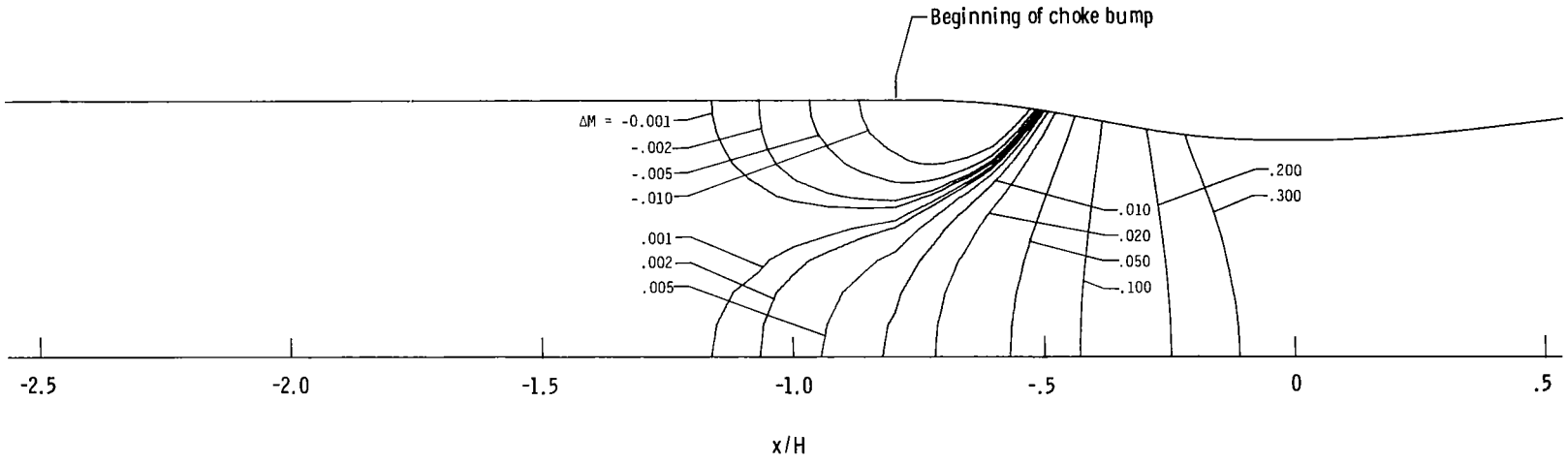

(e) $M_{nom} = 0.6$; $l/h = 10$.

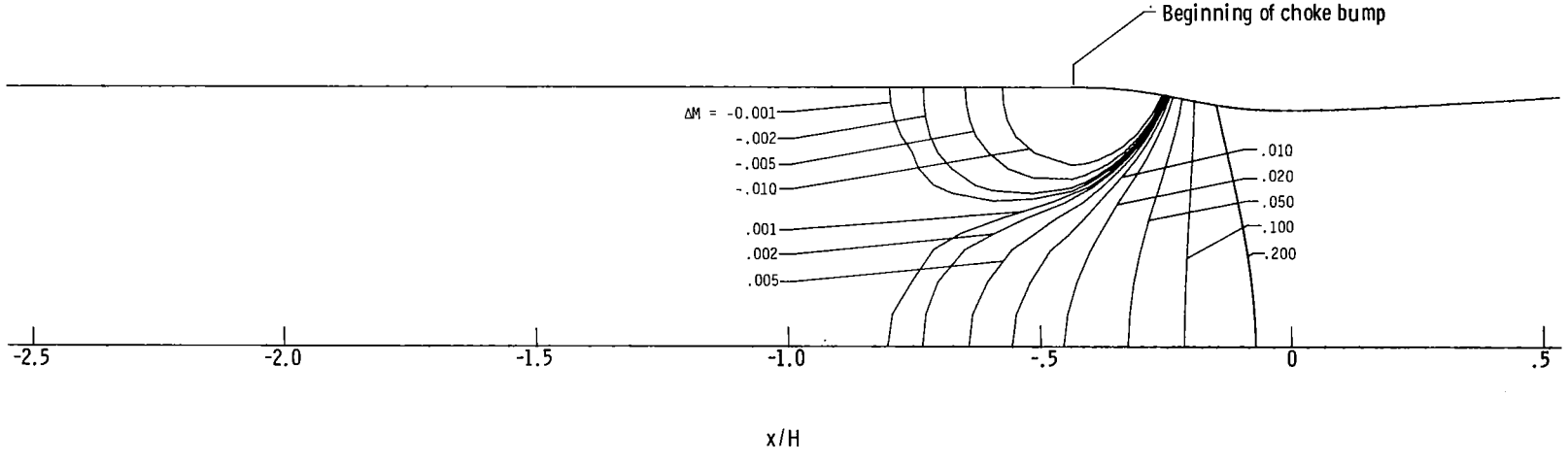

(f) $M_{nom} = 0.7$; $l/h = 10$.

Figure 6.- Continued.

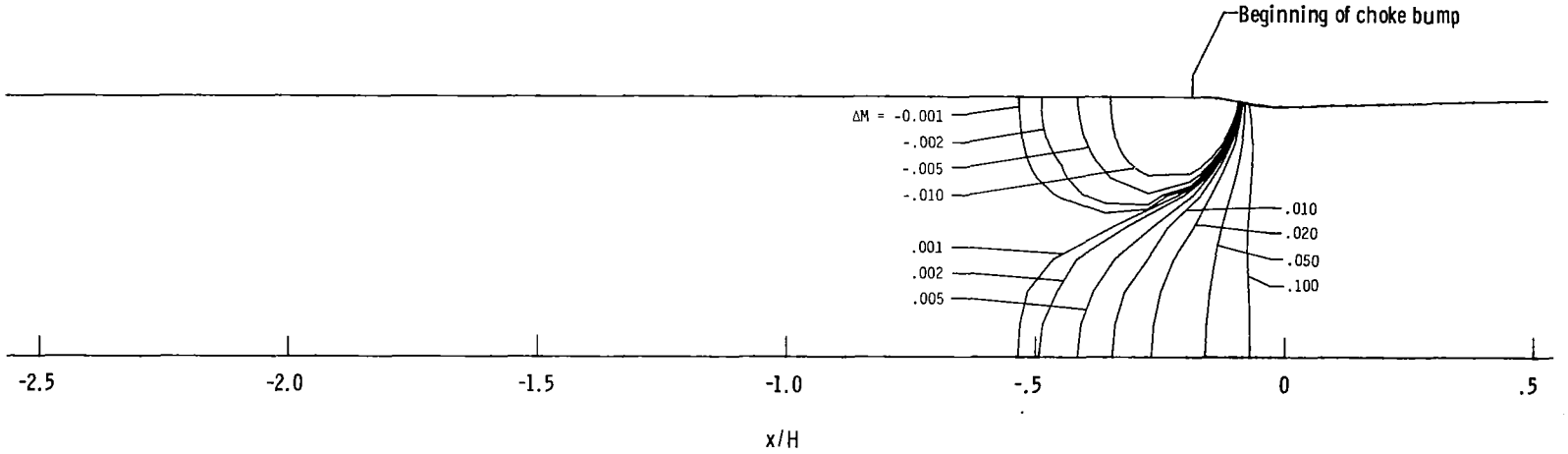

(g) $M_{nom} = 0.8$; $\ell/h = 10$.

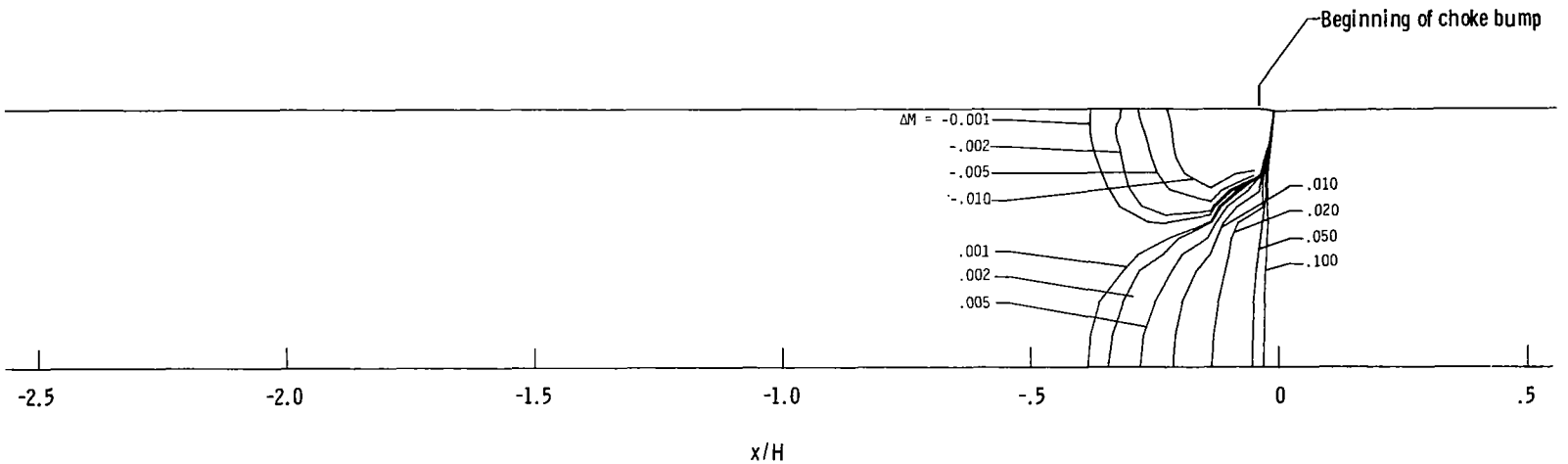

(h) $M_{nom} = 0.9$; $\ell/h = 10$.

Figure 6.- Concluded.

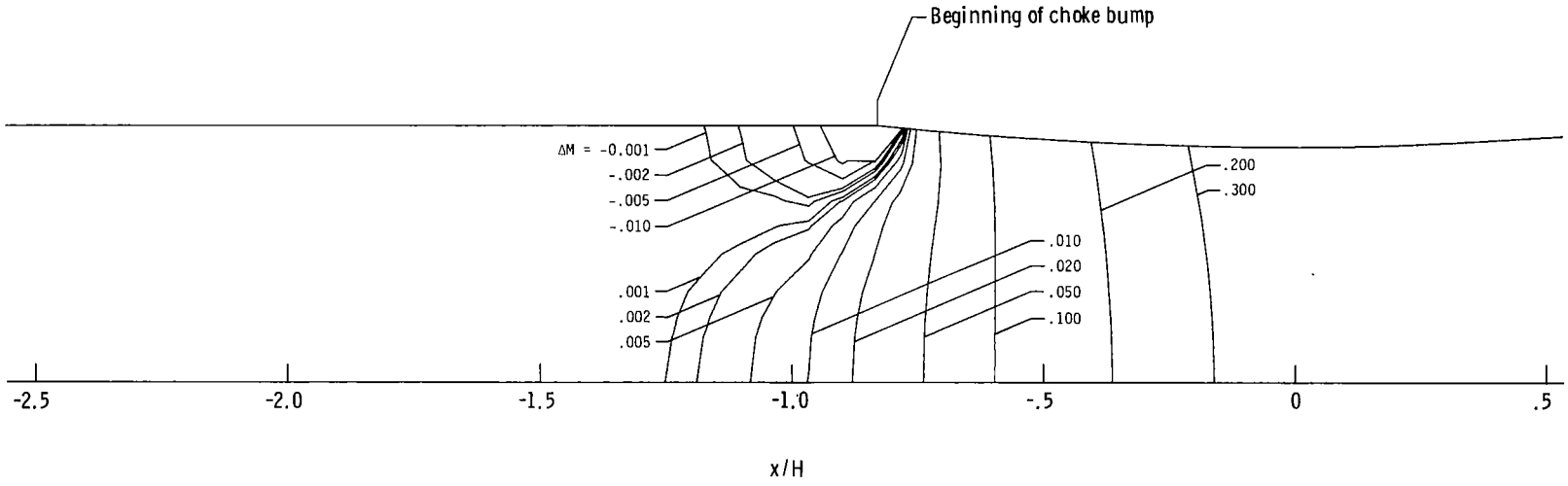

(a) $M_{nom} = 0.6$; $l/h = 20$.

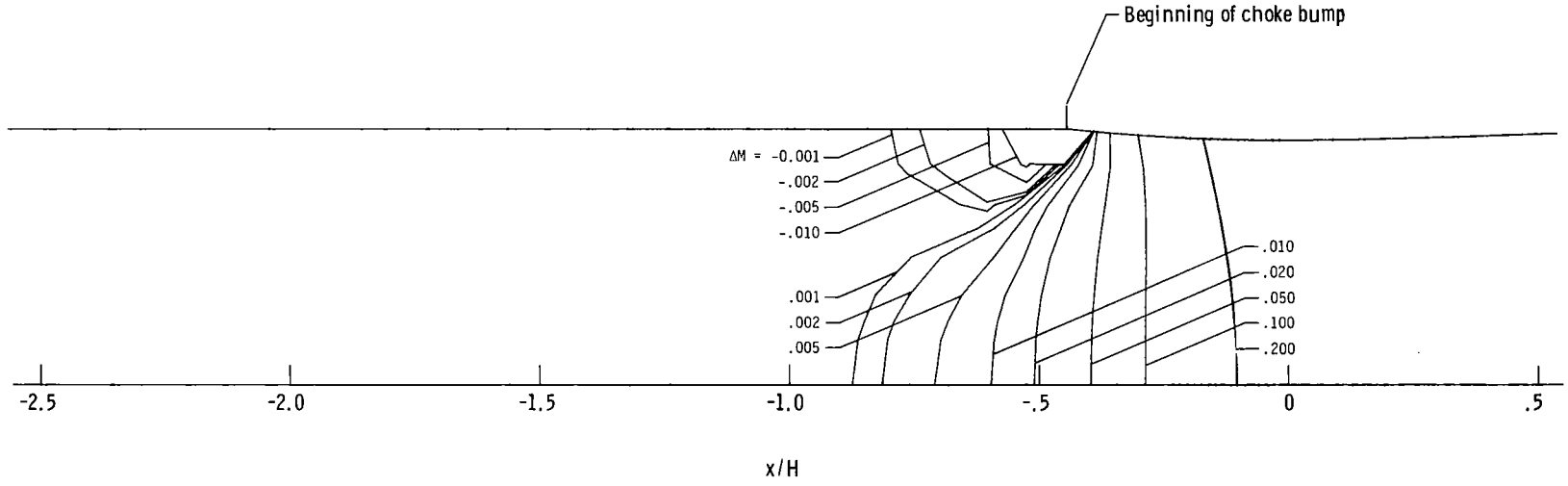

(b) $M_{nom} = 0.7$; $l/h = 20$.

Figure 7.- Mach number variation in tunnel for axisymmetric circular-arc choke bump cases.

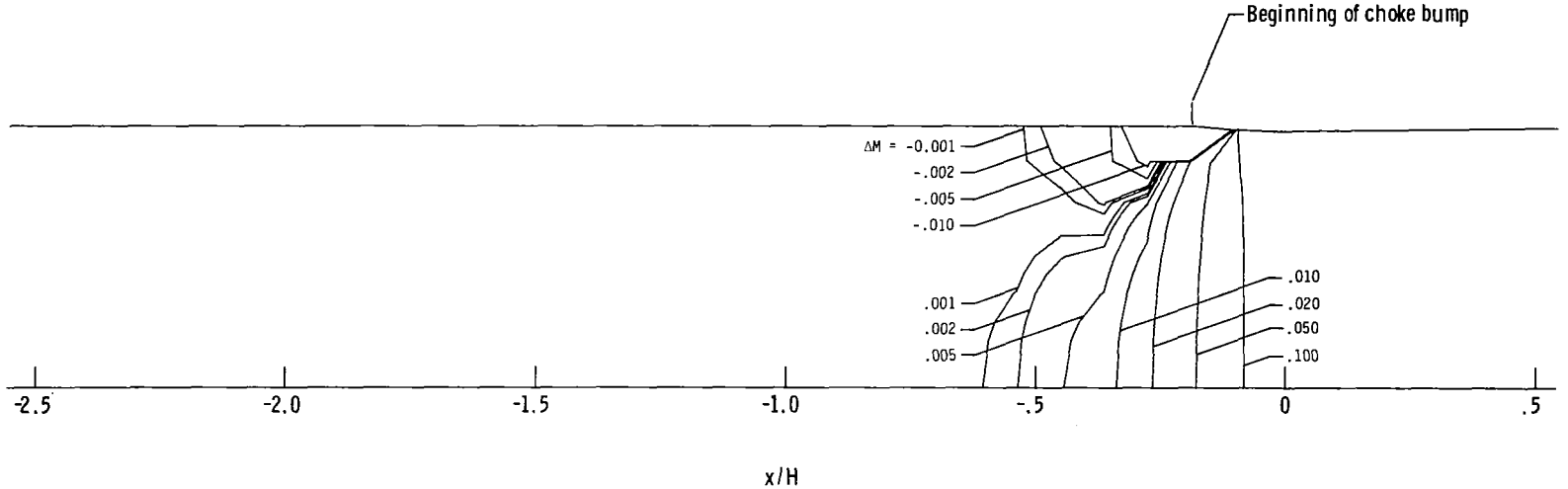

(c) $M_{nom} = 0.8$; $l/h = 20$.

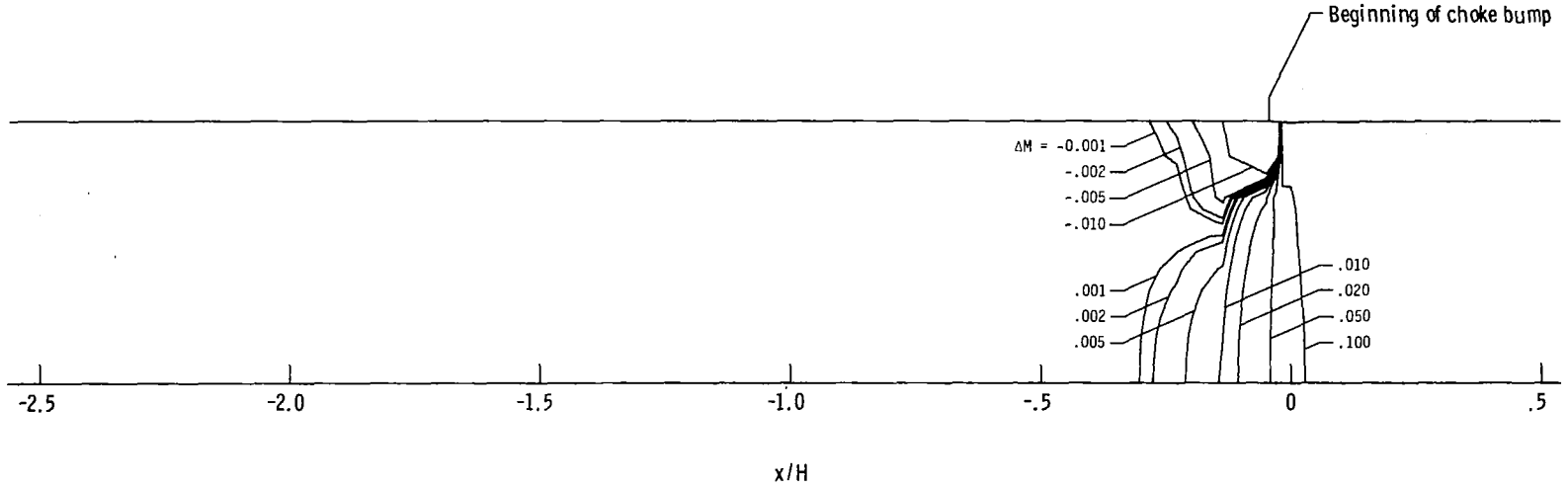

(d) $M_{nom} = 0.9$; $l/h = 20$.

Figure 7.- Continued.

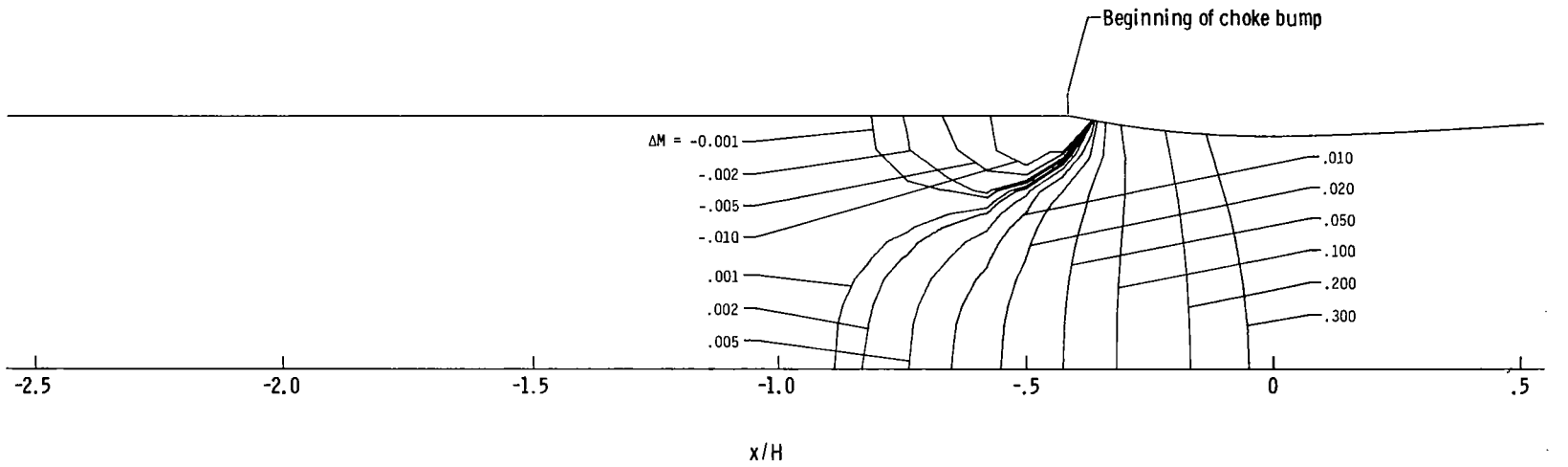

(e) $M_{nom} = 0.6$; $l/h = 10$.

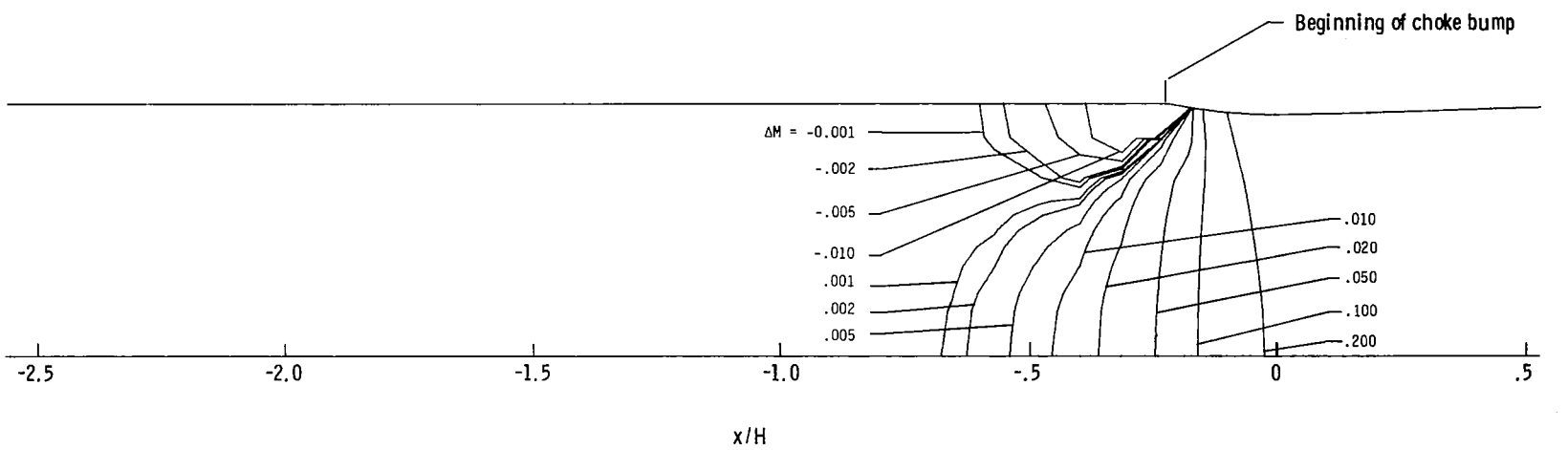

(f) $M_{nom} = 0.7$; $l/h = 10$.

Figure 7.- Continued.

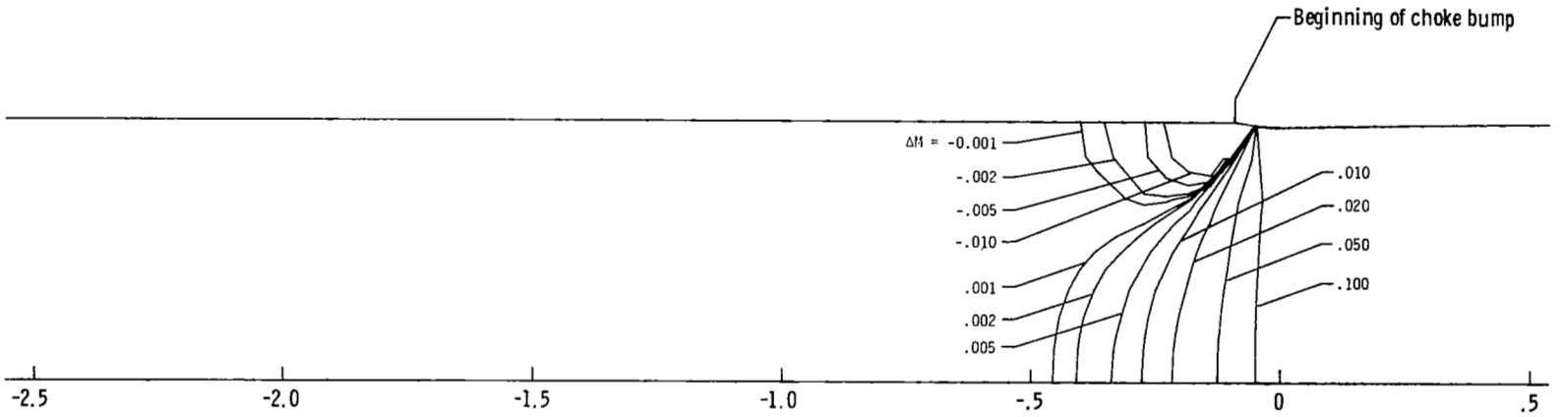

(g) $M_{nom} = 0.8$; $l/h = 10$.

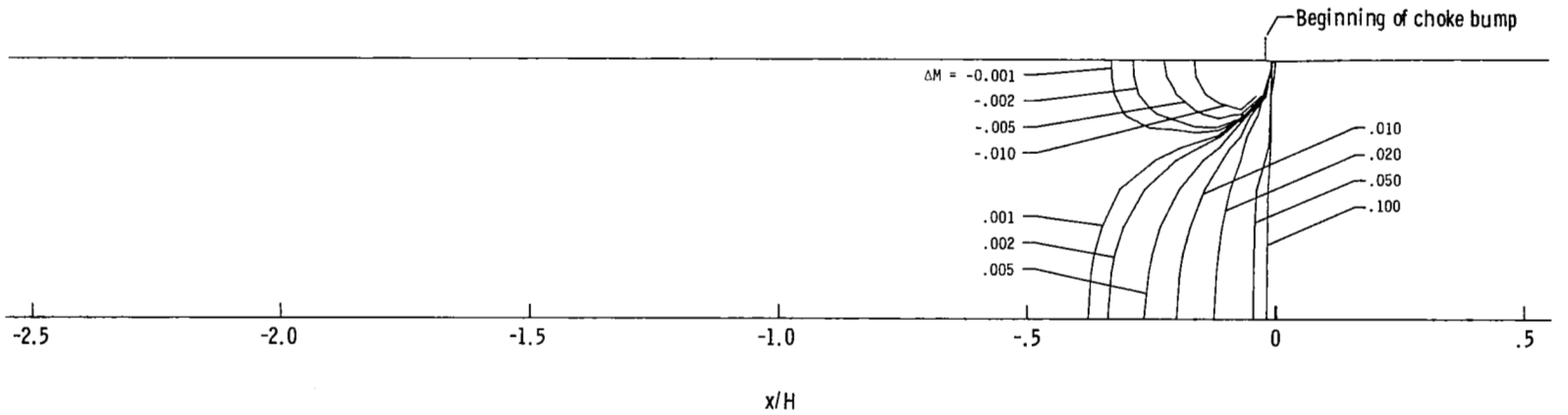

(h) $M_{nom} = 0.9$; $l/h = 10$.

Figure 7.- Concluded.

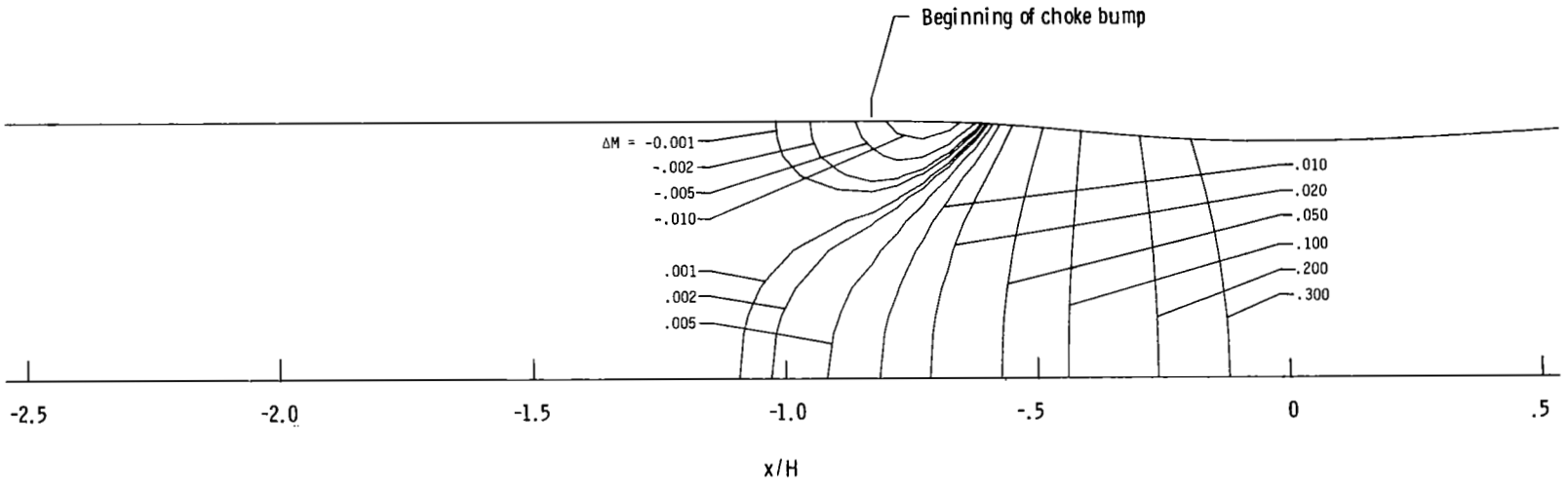

(a) $M_{nom} = 0.6$; $l/h = 20.$

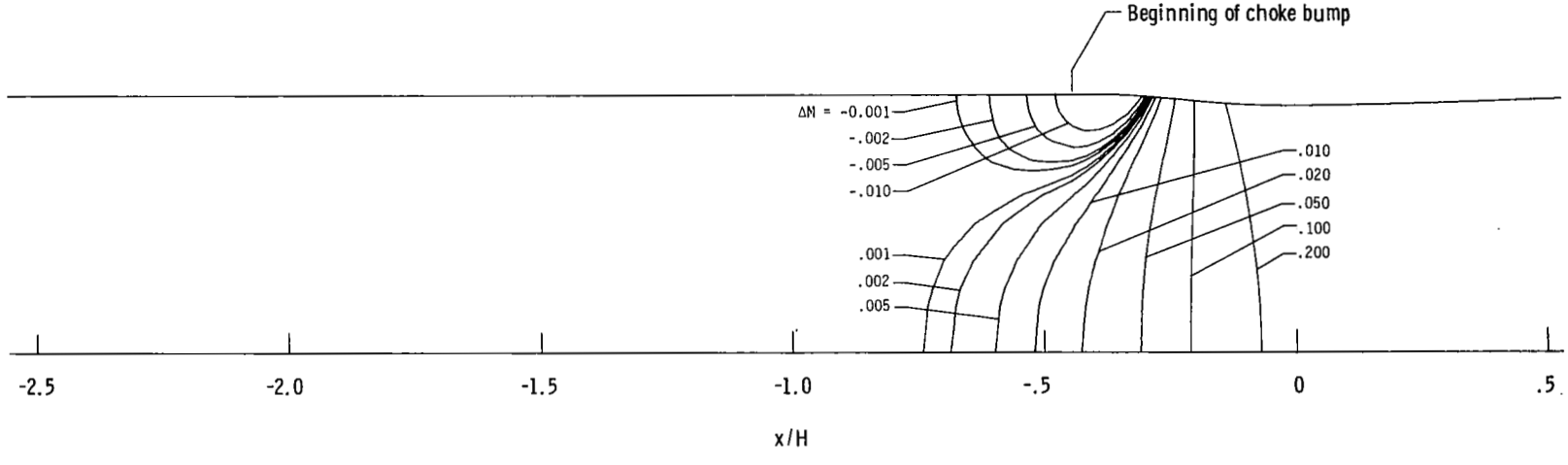

(b) $M_{nom} = 0.7$; $l/h = 20.$

Figure 8.- Mach number variation in tunnel for axisymmetric polynomial-curve choke bump cases.

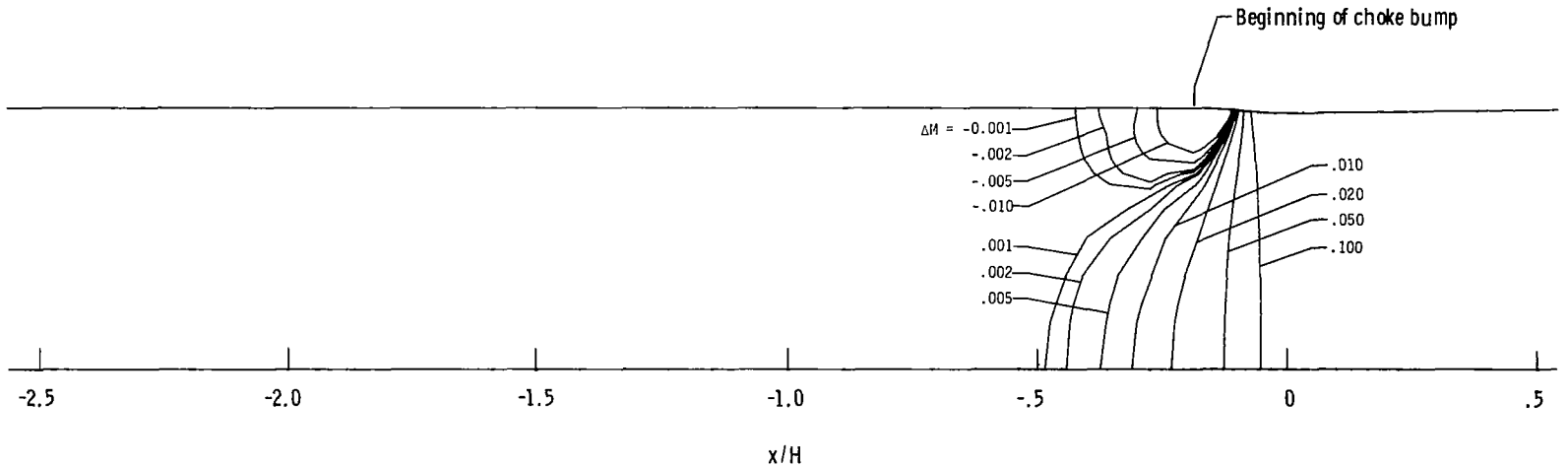

(c) $M_{nom} = 0.8$; $l/h = 20$.

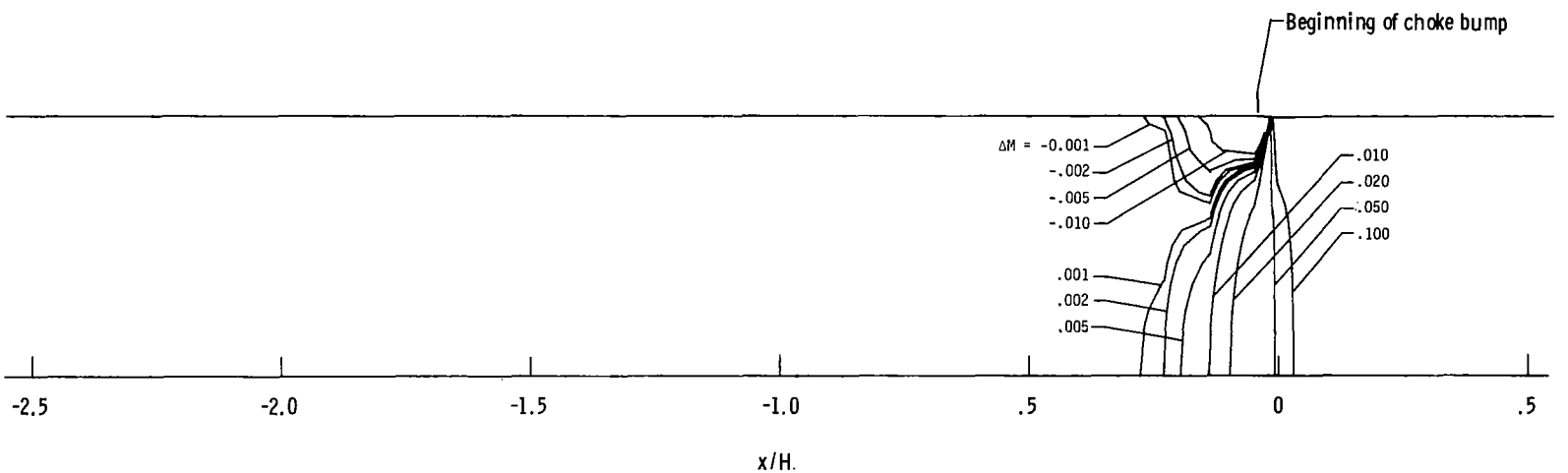

(d) $M_{nom} = 0.9$; $l/h = 20$.

Figure 8.- Continued.

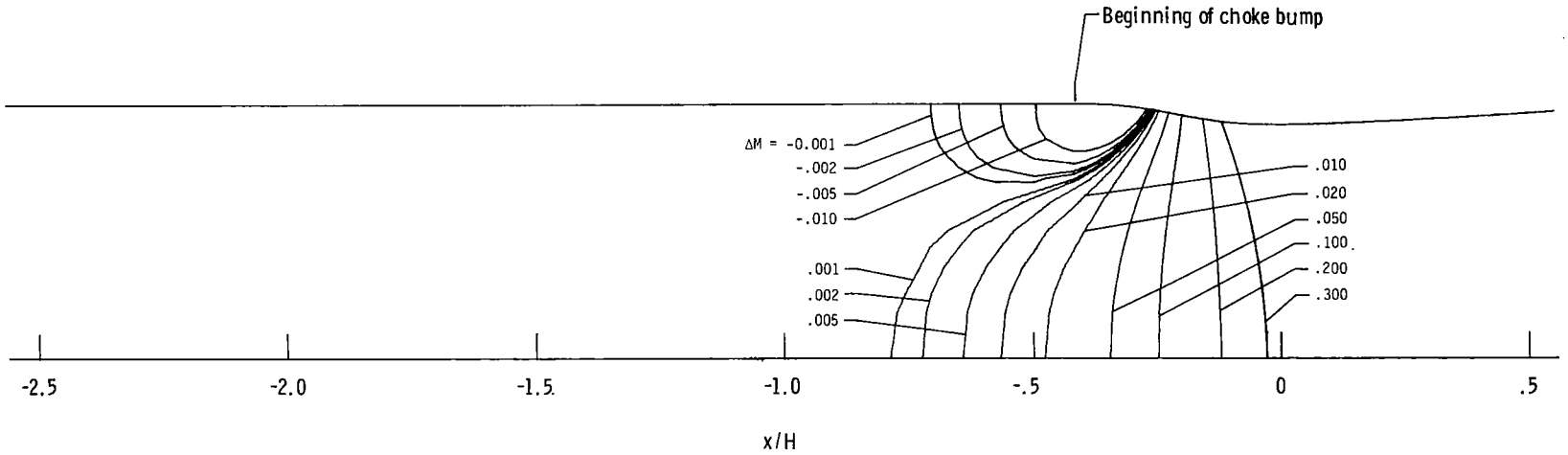

(e) $M_{nom} = 0.6$; $l/h = 10.$

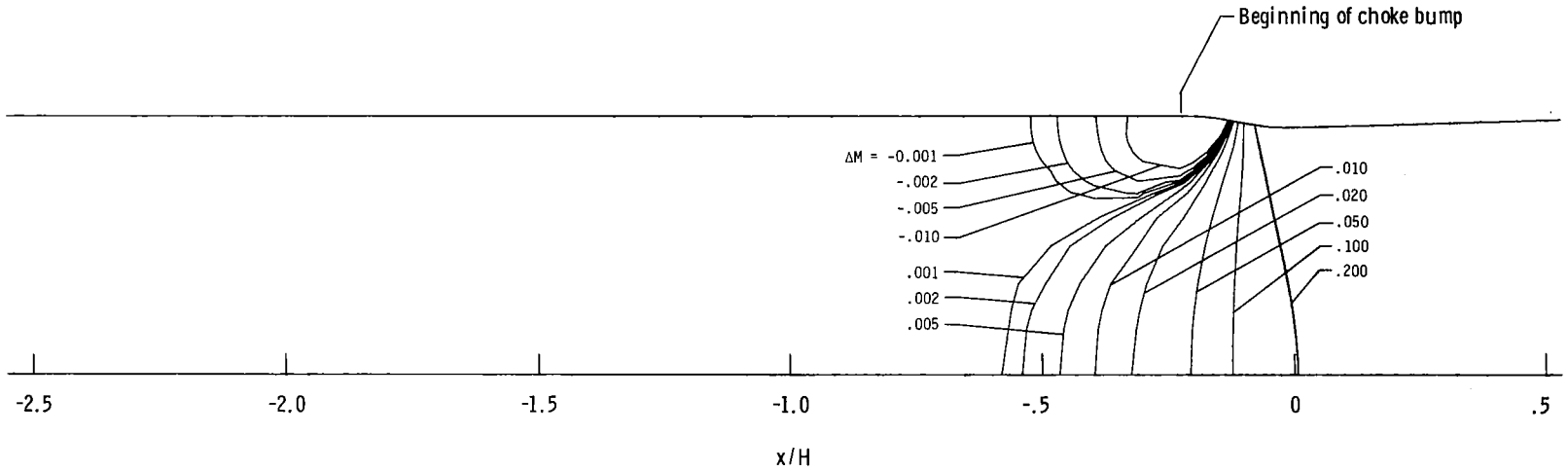

(f) $M_{nom} = 0.7$; $l/h = 10.$

Figure 8.- Continued.

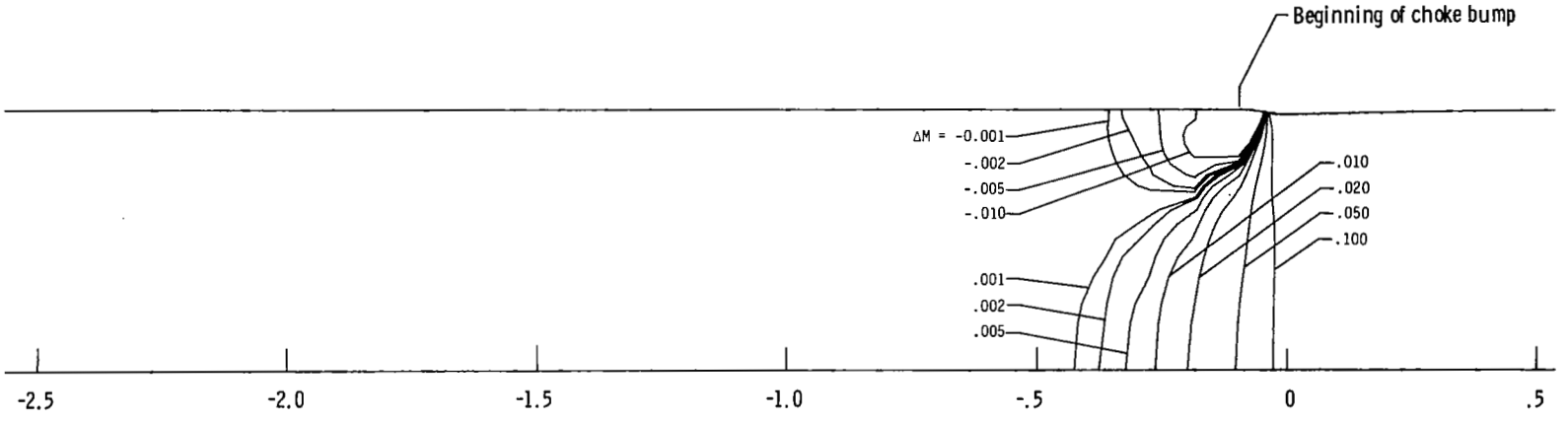

(g) $M_{nom} = 0.8$; $l/h = 10.$

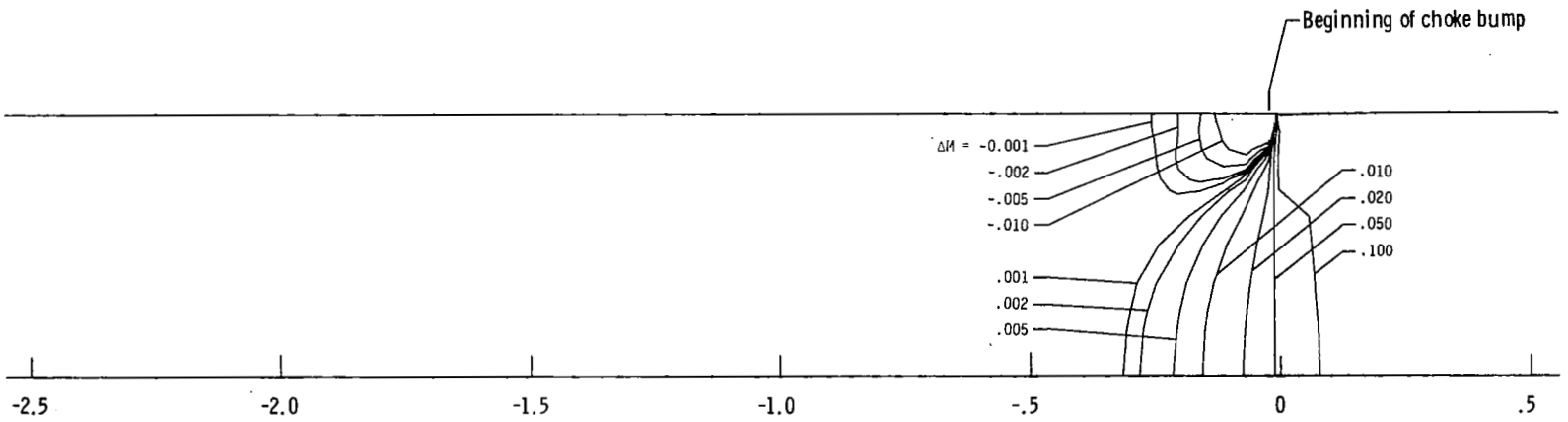

(h) $M_{nom} = 0.9$; $l/h = 10.$

Figure 8.- Concluded.

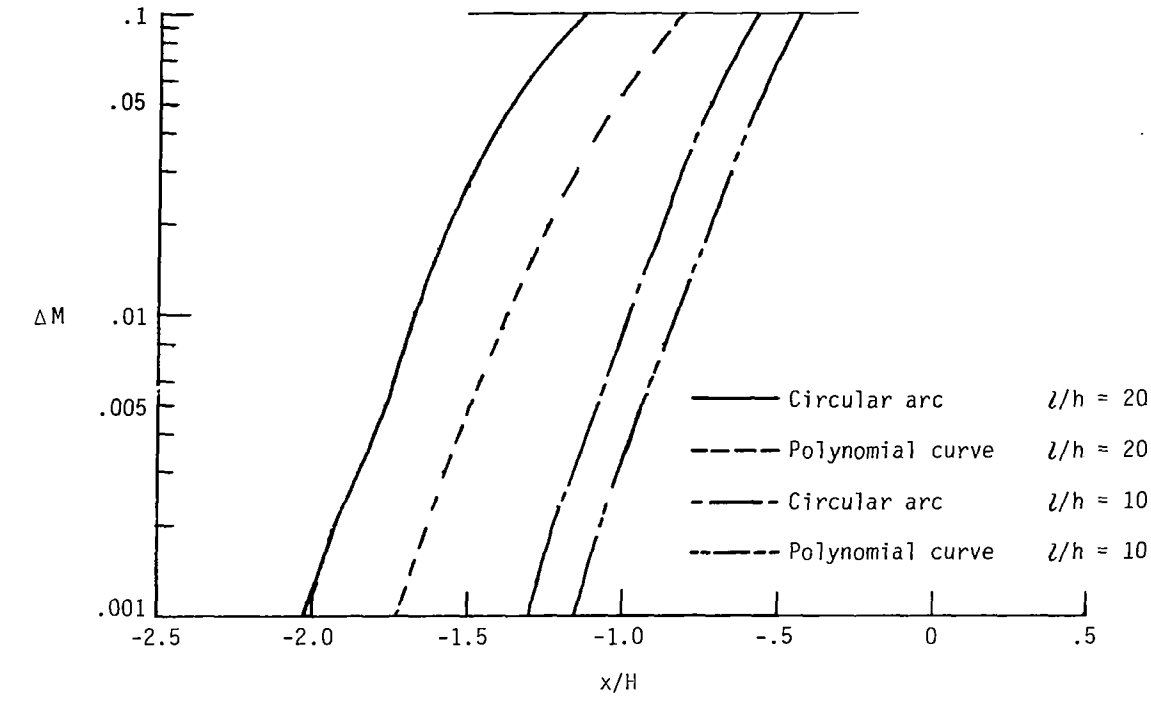

(a) $M_{nom} = 0.6$.

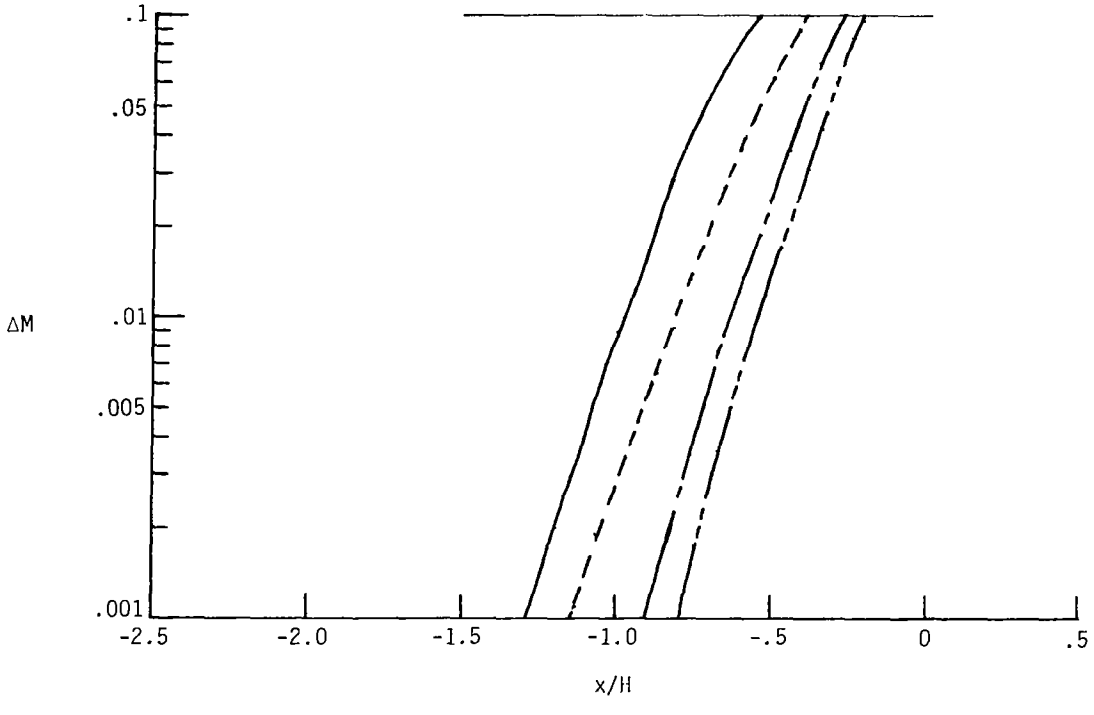

(b) $M_{nom} = 0.7$.

Figure 9.- Mach number variation along tunnel center line for two-dimensional cases.

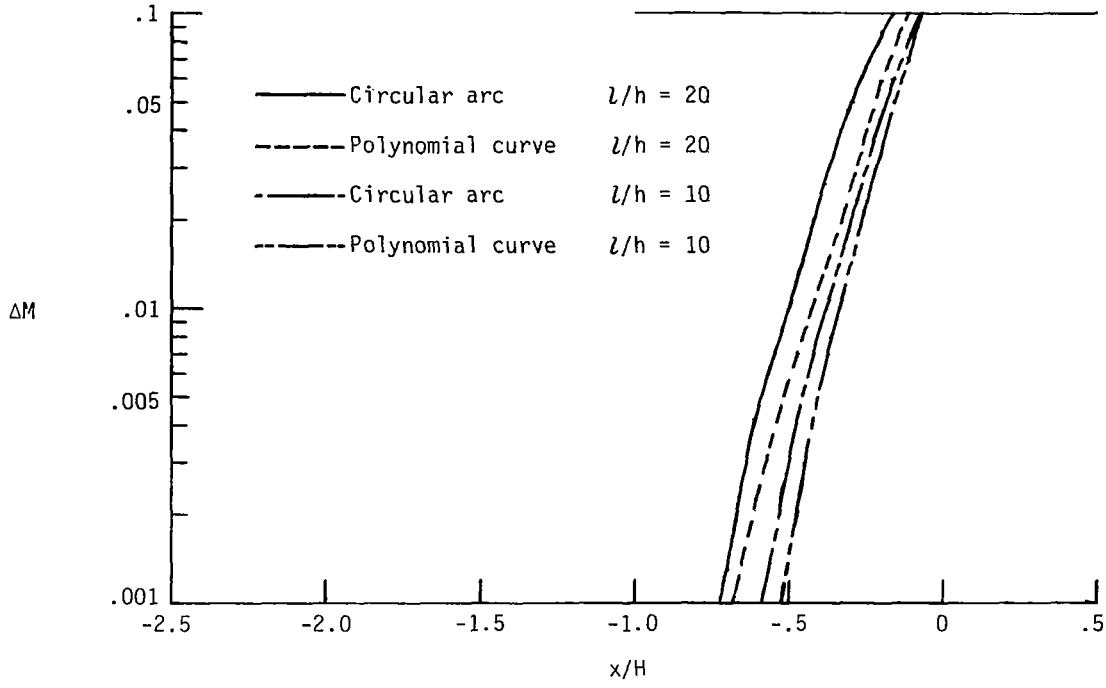

(c) $M_{nom} = 0.8$.

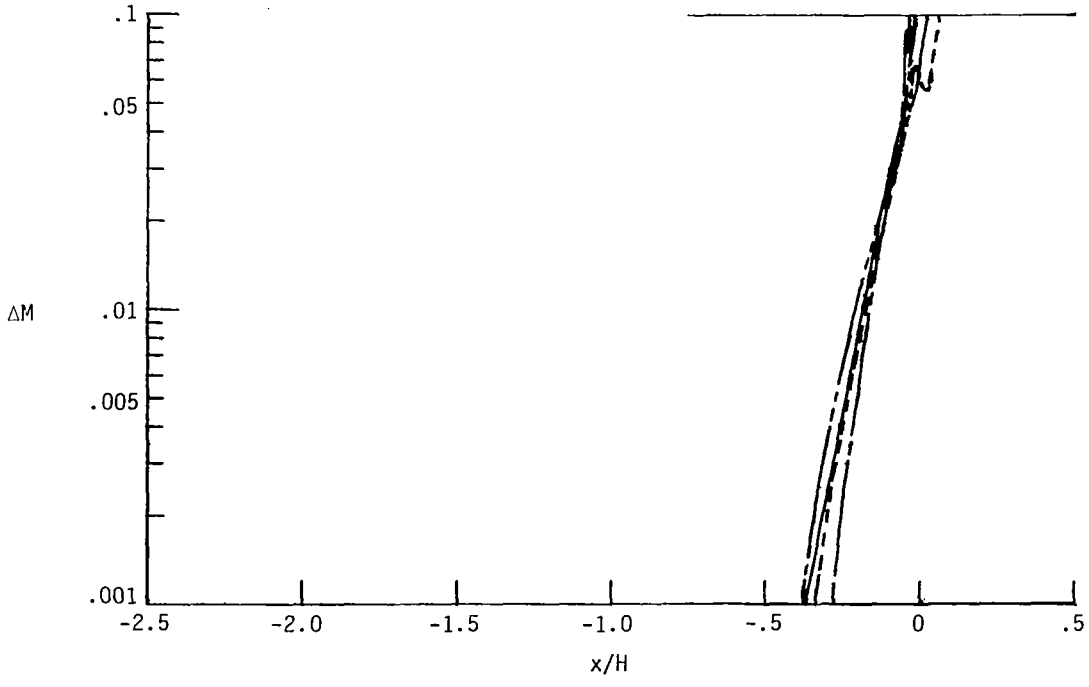

(d) $M_{nom} = 0.9$.

Figure 9.- Concluded.

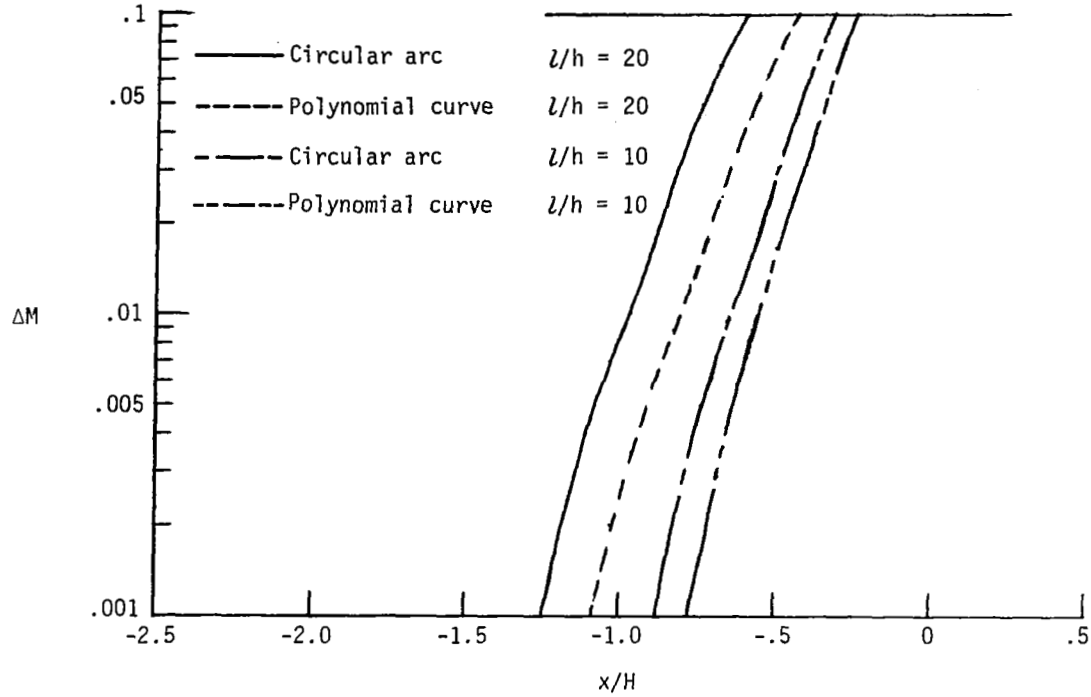

(a) $M_{nom} = 0.6$.

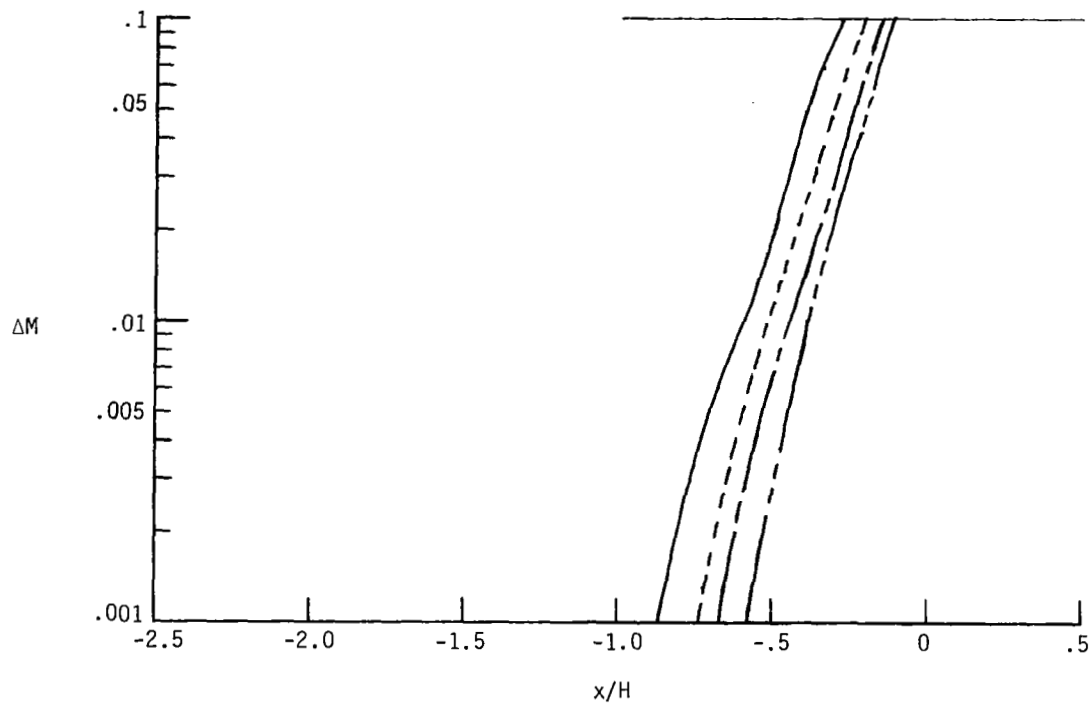

(b) $M_{nom} = 0.7$.

Figure 10.- Mach number variation along tunnel center line for axisymmetric cases.

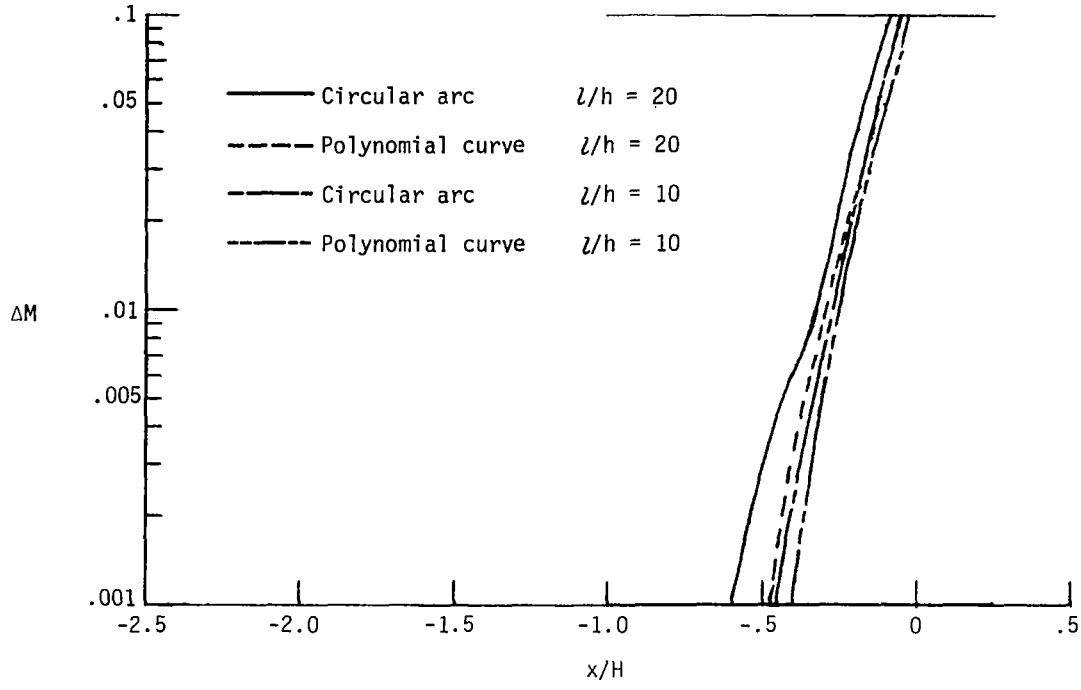

(c) M_{nom} = 0.8.

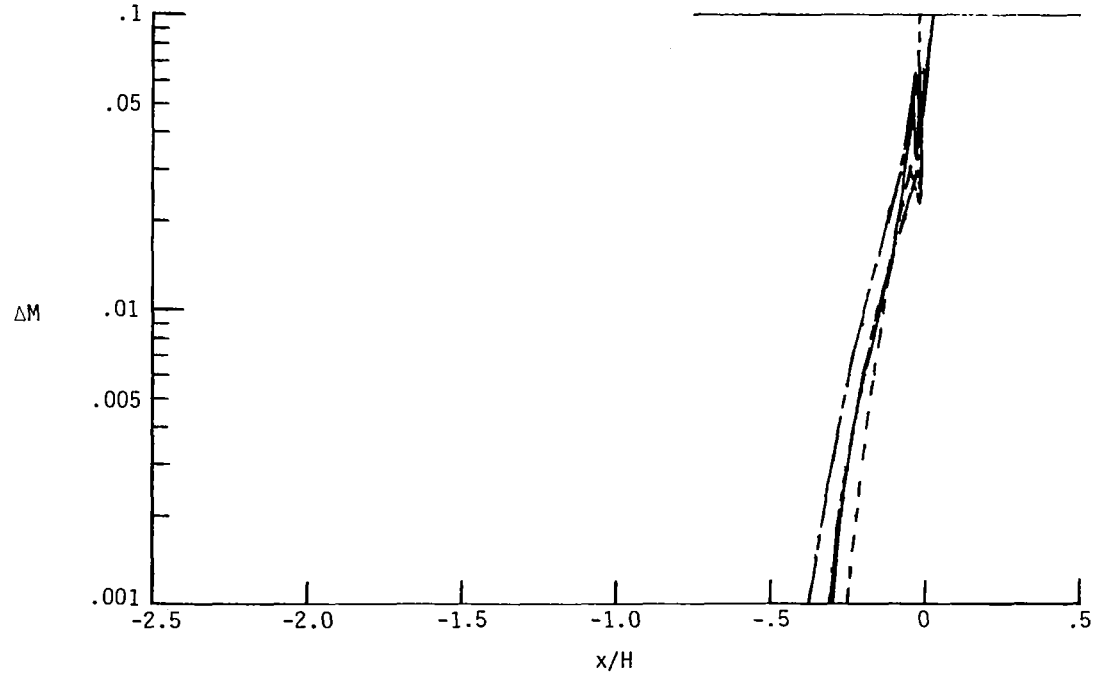

(d) M_{nom} = 0.9.

Figure 10.- Concluded.

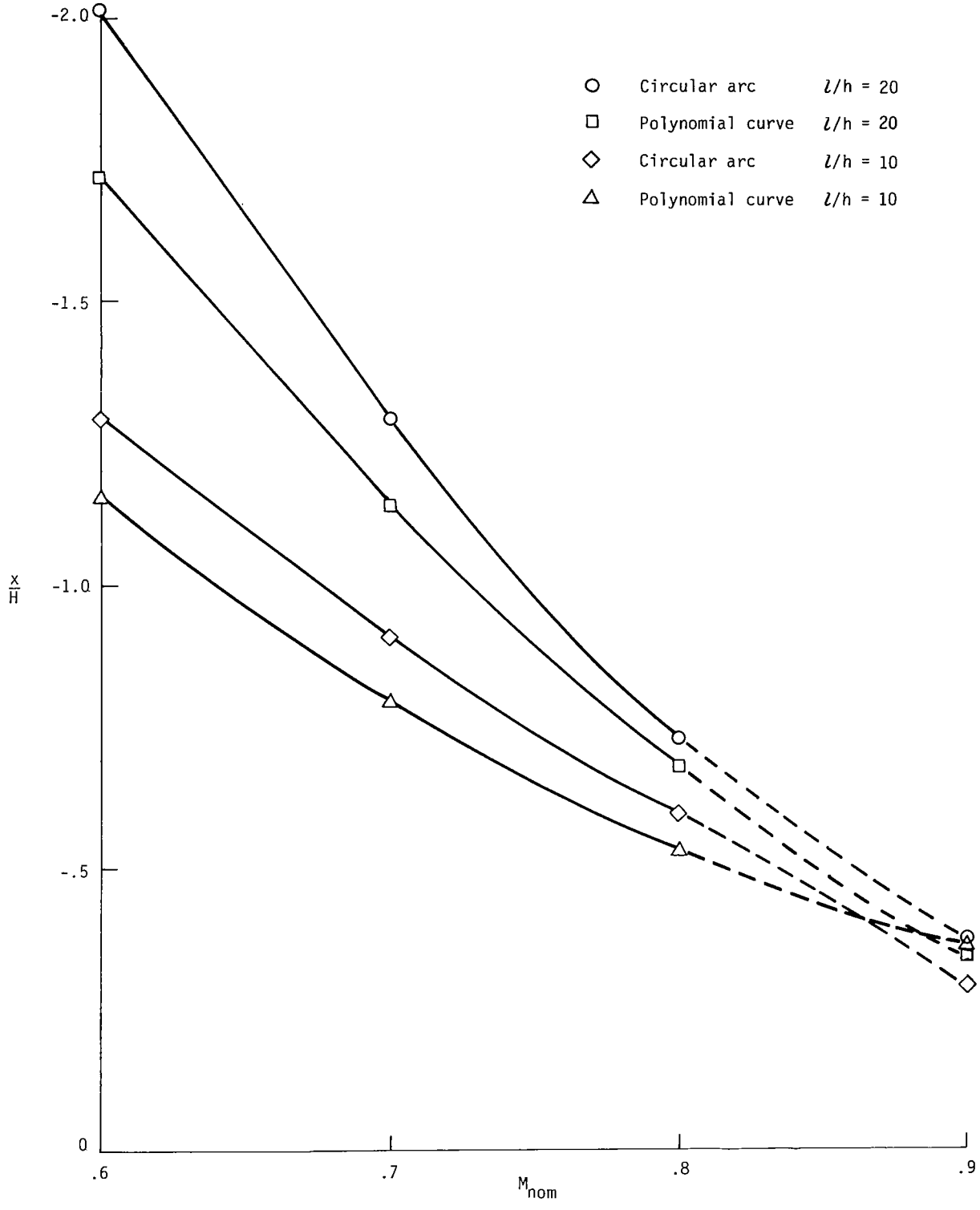

(a) Two-dimensional cases.

Figure 11.- Location of $\Delta M = 0.001$ perturbation level along tunnel center line.

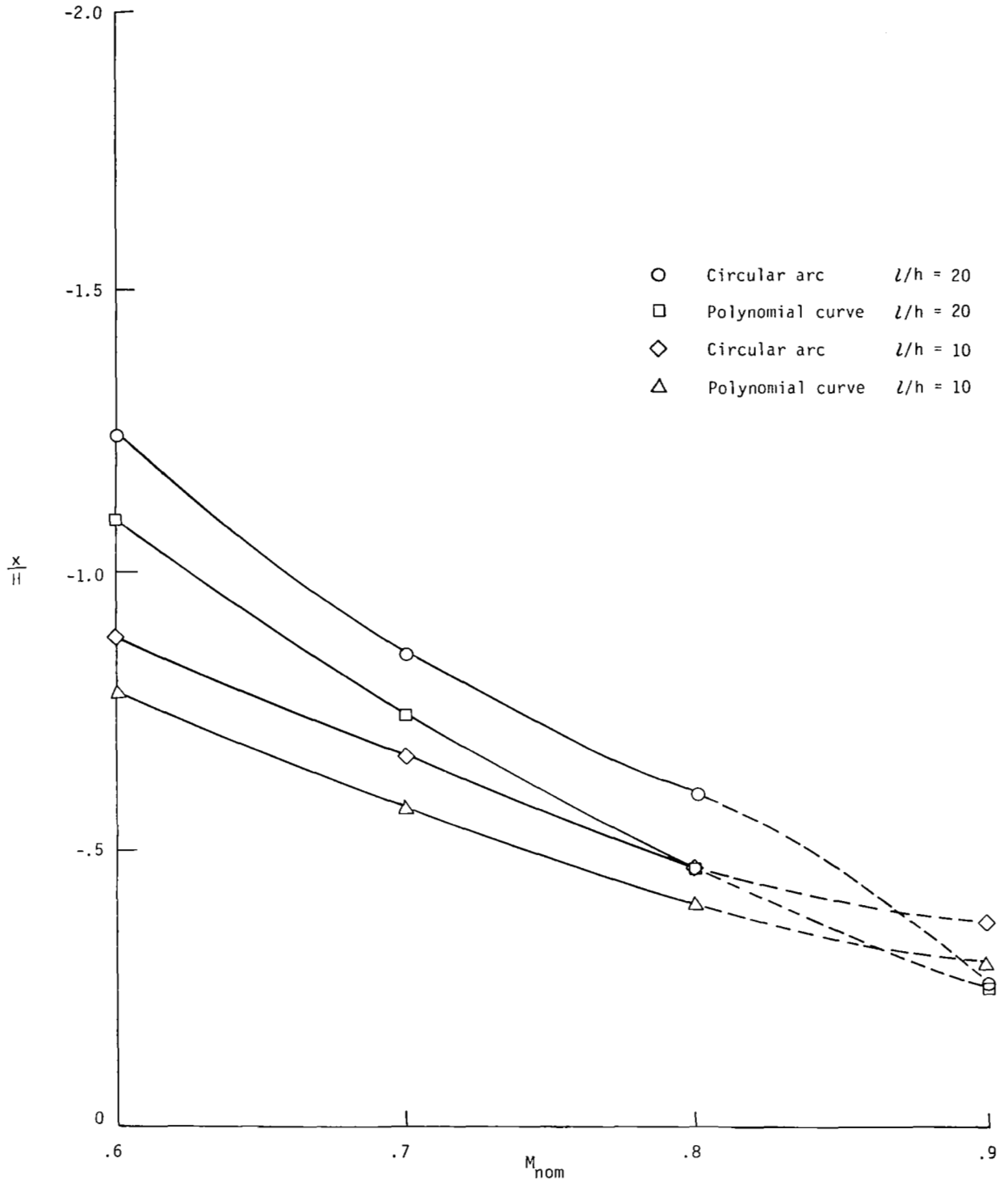

(b) Axisymmetric cases.

Figure 11.- Concluded.

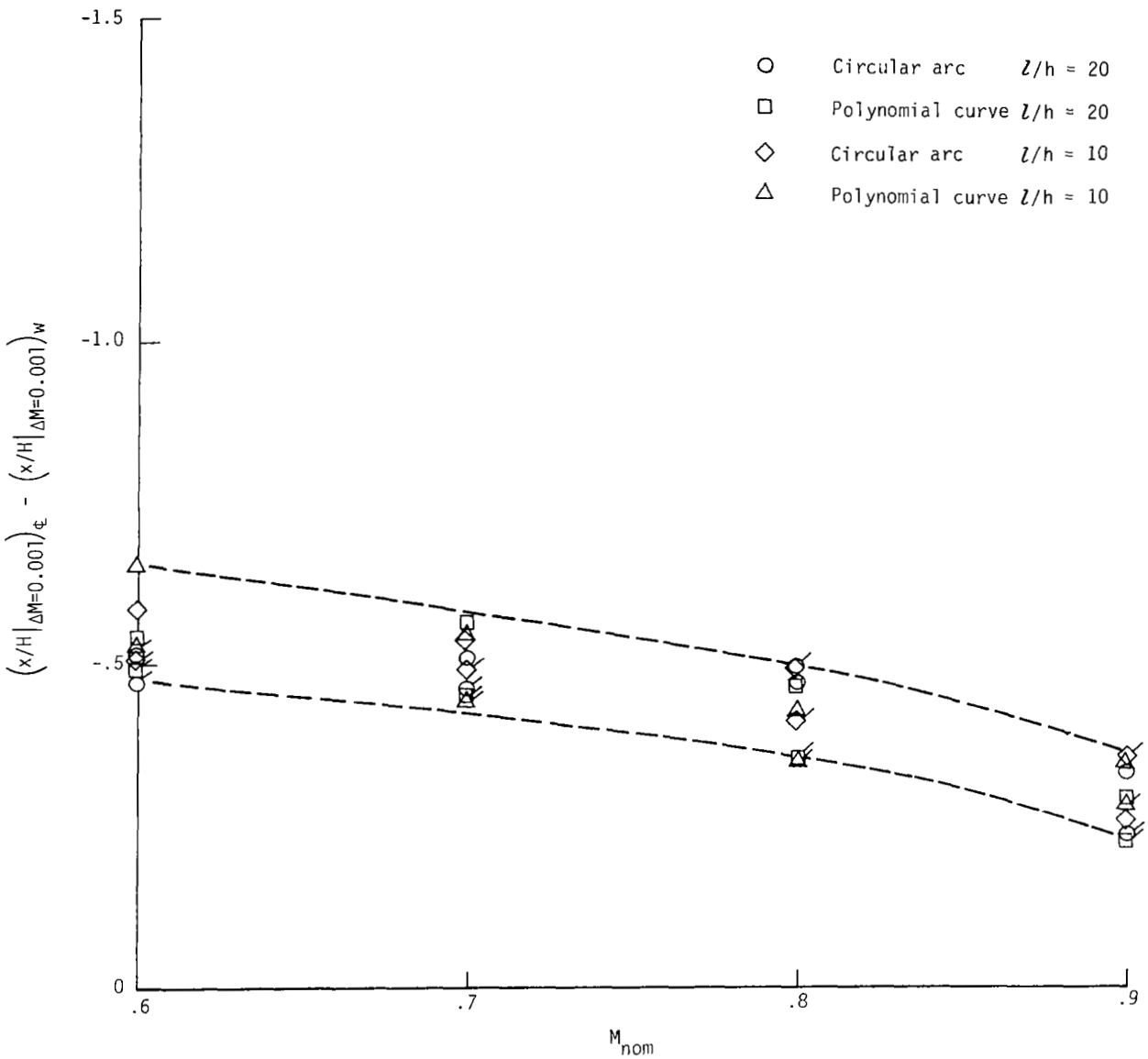

Figure 12.- Relative location of $\Delta M = 0.001$ perturbation level along tunnel center line. Flagged symbols are for axisymmetric cases.

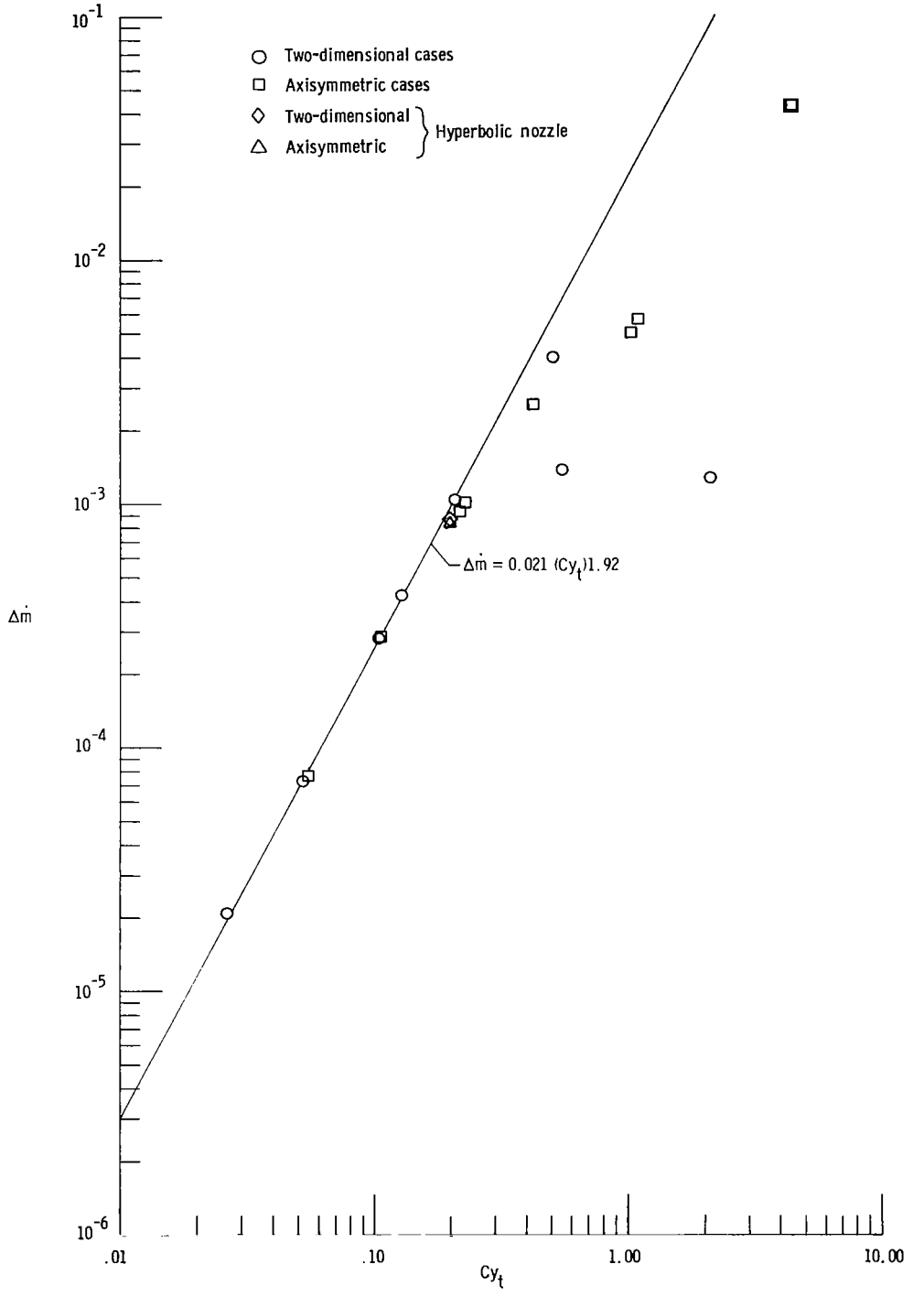

(a) Circular-arc cases.

Figure 13.- Correlation of mass-flow deficit with tunnel geometry parameter Cy_t.

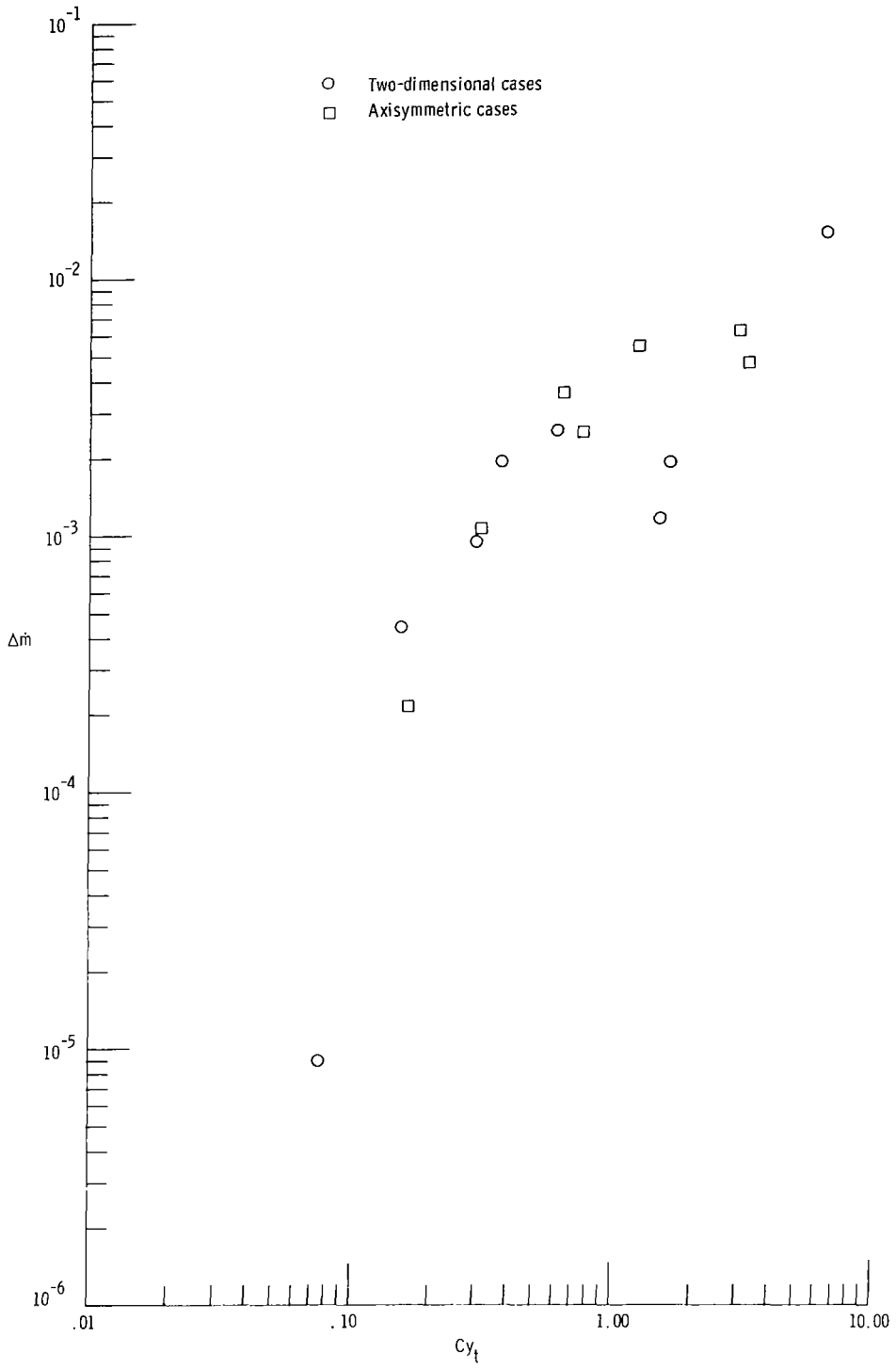

(b) Polynomial-curve cases.

Figure 13.- Concluded.

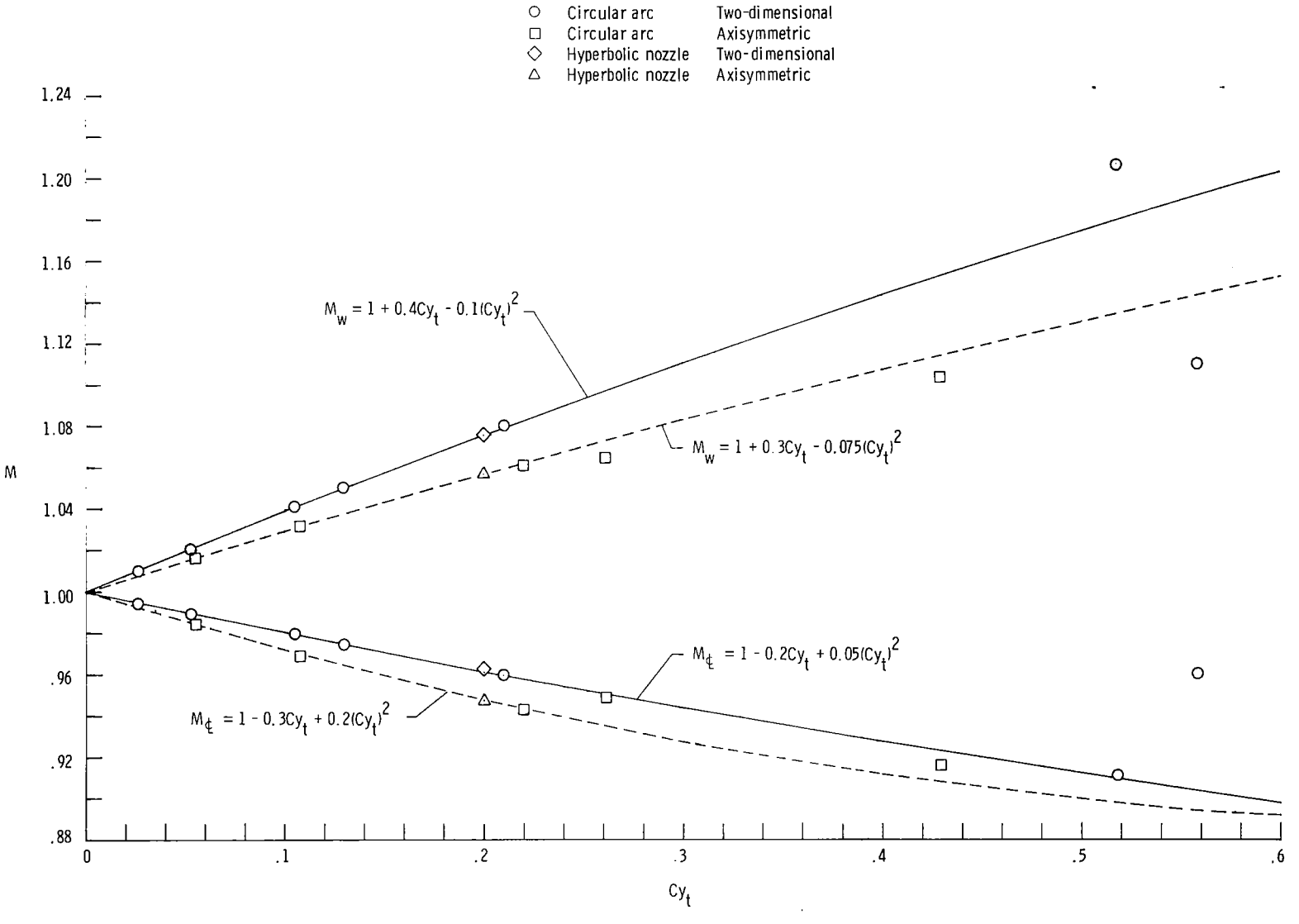

Figure 14.- Correlation of Mach numbers at tunnel throat with tunnel geometry parameter Cy_t.

1. Report No.	2. Government Accession No.	3. Recipient's Catalog No.
NASA TP-1892		

4. Title and Subtitle	5. Report Date
COMPUTER ANALYSIS OF FLOW PERTURBATIONS GENERATED BY PLACEMENT OF CHOKE BUMPS IN A WIND TUNNEL	August 1981
	6. Performing Organization Code: 505-43-23-06
7. Author(s): Richard L. Campbell	8. Performing Organization Report No.: L-14415
9. Performing Organization Name and Address: NASA Langley Research Center, Hampton, VA 23665	10. Work Unit No.
	11. Contract or Grant No.
12. Sponsoring Agency Name and Address: National Aeronautics and Space Administration, Washington, DC 20546	13. Type of Report and Period Covered: Technical Paper
	14. Sponsoring Agency Code

15. Supplementary Notes

16. Abstract

An inviscid analytical study has been conducted to determine the upstream flow perturbations caused by placing choke bumps in a wind tunnel. A computer program based on the stream-tube curvature method was used to calculate the resulting flow fields for a nominal free-stream Mach number range of 0.6 to 0.9. The choke bump geometry was also varied to investigate the effect of bump shape on the disturbance produced. Results from the study indicate that a region of significant variation from the free-stream conditions exists upstream of the throat of the tunnel. The extent of the disturbance region was, as a rule, dependent on Mach number and the geometry of the choke bump. In general, the upstream disturbance distance decreased for increasing nominal free-stream Mach number and for decreasing length-to-height ratio of the bump. A polynomial-curve choke bump usually produced less of a disturbance than did a circular-arc bump, and going to an axisymmetric configuration (modeling choke bumps on all the tunnel walls) generally resulted in a lower disturbance than with the corresponding two-dimensional case.

17. Key Words (Suggested by Author(s))	18. Distribution Statement
Choke bumps Wind-tunnel flow quality Choked tunnel	Unclassified - Unlimited Subject Category 02

19. Security Classif. (of this report)	20. Security Classif. (of this page)	21. No. of Pages	22. Price
Unclassified	Unclassified	42	A03

For sale by the National Technical Information Service, Springfield, Virginia 22161

NASA-Langley, 1981